Title: Dopamine D1 receptor expression in dlPFC inhibitory parvalbumin neurons may contribute to higher visuospatial distractibility in marmosets versus macaques

Authors: Joyce MKP[*1], Ivanov TG[*2], Krienen FM[3,4], Mitchell JF[5], Ma S[1,17], Inoue W[6,7], Nandy AS[1,8,9], Datta D[10], Duque A[1], Arellano J[1], Gupta R[2], Gonzalez-Burgos G[11], Lewis DA[11,12], Sestan N[1,8,12,13], McCarroll SA[4,14], Martinez-Trujillo J[6,7,15,16], Froudist-Walsh S[2+], Arnsten AFT[1,8,9+]

Affiliations:
*-co-first authorship/equal contributions
+corresponding authors
1-Department of Neuroscience, Yale University School of Medicine, New Haven, CT 06510, USA
2- School of Engineering, Mathematics & Technology, University of Bristol, Bristol, UK
3-Princeton Neuroscience Institute, Princeton University, Princeton, NJ 08544, USA
4-Department of Genetics, Harvard Medical School, Boston, MA 02115, USA
5-Department of Brain and Cognitive Sciences, University of Rochester, New York, NY 14627, USA
6-Robarts Research Institute, Western University, London ON N6A 5K8, Canada
7-Department of Physiology and Pharmacology, Schulich School of Medicine and Dentistry, University of Western Ontario, London, ON N6A 5C1, Canada
8-Wu Tsai Institute, Yale University, New Haven, CT 06510, USA
9-Kavli Institute for Neuroscience, Yale University School of Medicine, New Haven, CT 06510, USA
10-Department of Psychiatry, Yale University School of Medicine, New Haven, CT 06510, USA
11-Department of Psychiatry, University of Pittsburgh, Pittsburgh, PA 15260, USA
12-Department of Neuroscience, University of Pittsburgh, Pittsburgh, PA 15213, USA
13-Department of Genetics and Comparative Medicine, Program in Cellular Neuroscience, Neurodegeneration and Repair, and Yale Child Study Center, Yale University School of Medicine, New Haven CT 06510, USA
14-Stanley Center for Psychiatric Research, Broad Institute of MIT and Harvard, Cambridge, MA 02142, USA
15-Department of Psychiatry, Schulich School of Medicine and Dentistry, University of Western Ontario, London, ON N6A 5C1, Canada
16-Western Institute for Neuroscience, University of Western Ontario, London, ON N6A 3K7, Canada
17- Institute of Neuroscience, CAS Center for Excellence in Brain Science and Intelligence Technology, University of Chinese Academy of Sciences, Chinese Academy of Sciences, Shanghai 200031, China

Corresponding authors:
Dr. Amy F.T. Arnsten, Albert E. Kent Professor of Neuroscience
Dept. Neuroscience, Yale Medical School
333 Cedar St., New Haven, CT USA 06510
Email: amy.arnsten@yale.edu
Phone: 203-785-4431 Mobile: 203-530-3954 FAX: 203-785-5263

Dr. Seán Froudist-Walsh
School of Engineering, Mathematics & Technology, University of Bristol
BS8 1UB, Bristol, UK
Email: sean.froudist-walsh@bristol.ac.uk
Phone: +447541515541

Acknowledgements:
This research was funded by NSF 2015276 to AFTA, JMT, FMK and SAM, as well as by a Bristol Neuroscience of Mental Health award (co-funded by Steve Scobie and Anne Graham) and BBSRC BB/X013243/1 to SFW. We thank the Yale Center for Cellular & Molecular Imaging Confocal Facility for usage of their Zeiss LSM 880 Airyscan microscope. The modelling work was carried out using the high-performance computing facilities of the Advanced Computing Research Centre, University of Bristol – http://www.bristol.ac.uk/acrc/. We are grateful to Kristy Gibbs, Lisa Ciavarella, Tracy Sadlon, Sam Johnson, and Michelle Wilson for their technical expertise. Additionally, we thank Albert Compte, Joao Barbosa, Paul Anastasiades, John Hongyu Meng, and Christos Constantinidis for helpful discussions, as well as Matt Jones, Ulysse Klatzmann, Aswathi Thrivikraman, Dabal Pedamonti, and Eva Sevenster for feedback on the manuscript. Further thanks to Benjamin Corrigan and Diego Buitrago-Piza for their behavioral task illustrations, which we have adapted for Figure 1.

Abstract:
Marmosets and macaques are common non-human primate models of cognition, but evidence suggests that marmosets perform more poorly and appear more distractible during cognitive tasks. Prior experimental and theoretical work in macaques suggests that dopaminergic modulation and inhibitory parvalbumin (PV) neurons could contribute to distractibility during cognitive performance. Thus, we compared the two species using a visual fixation task with distractors, performed molecular and anatomical analyses in the dorsolateral prefrontal cortex (dlPFC), and linked functional microcircuitry with cognitive performance using computational modeling. We found that marmosets are indeed more distractible than macaques, and that marmoset dlPFC PV neurons contain higher levels of dopamine-1 receptor (D1R) transcripts and protein. The computational model suggested that higher D1R expression in marmoset dlPFC PV neurons may induce distractibility within the typical, mid D1R stimulation range. Our interdisciplinary study can inform species choice for translational studies of cognition, and clarify microcircuit mechanisms for distractor resistance.

Declaration of Interests: The authors have nothing to declare.

Author Contributions: AFTA, MKPJ, TGI, and SFW designed the study; MKPJ collected and analyzed anatomical data; TGI, RG, and SFW designed and performed the modeling; FM and SAM collected and analyzed transcriptomics data; GGB and DAL provided macaque brain tissue for transcriptomics performed by FM; SM and NS collected and analyzed phylogenetic transcriptomics dataset; JFM and ASN performed and analyzed the behavioral testing; IW and JMT provided the marmoset tissue for immunofluorescence; MKPJ, TGI, SFW, and AFTA wrote the first draft and all authors revised and edited subsequent drafts of the article.

Introduction

Marmosets are an increasingly attractive non-human primate model due to their small size, ease of handling, short breeding cycle, brief lifespan, and amenability to emerging genetic and molecular technologies (e.g.,[1]). The use of marmosets has already proven successful in modeling many psychiatric and mental processes[2-4]. Yet the extent of their translational validity and similarity to macaques in cognitive domains is still under investigation, as very few studies have directly compared the two species in the same tasks. One early study[5] found that marmosets required more trials to match macaque performance on a delayed-response working memory task, and marmoset performance, compared to that of macaques, worsened more with longer delays. Additionally, marmosets invariably failed the task if they became distracted away from the screen, while macaques could overcome external distractions and respond correctly[5]. More recently, assays of attentional regulation show that macaques[6] have a superior ability to regulate attention shifting compared to marmosets[7]. These data are consistent with anecdotal reports that high levels of distractibility in marmosets can interfere with training[8]. Although a more comprehensive comparison of cognitive abilities across these species remains necessary, the evidence suggests that marmosets perform more poorly in tasks with higher cognitive demands, and that they may be more susceptible than macaques to distractibility, which we define as overt behavioral responses to external task-irrelevant stimuli. These cross-species differences in cognitive function necessitate a comparison of the neural circuitry supporting these processes in marmosets and macaques.

Core cognitive processes, such as working memory and attention, may rely on partially overlapping neuronal populations in the dlPFC[9, 10], although others have argued for more dissociation[11]. Studies of macaque dlPFC have revealed that extensive recurrent excitation among pyramidal neurons in specialized microcircuits of deep layer III maintains persistent firing activity across a working memory delay period, even in the presence of distractors[12, 13]. These layer III pyramidal neurons, known as Delay cells, are considered essential for maintaining mental representations in the absence of external stimuli. Inhibitory, GABAergic PV neurons have also been central to early theories of the cellular basis of attention and working memory[12-14], though their exact contributions to cognitive function and particularly distractibility are still unclear. Evidence suggests that fast-spiking, putative PV neurons may be actively recruited during the delay period to sculpt the spatial tuning of excitatory Delay cell activities[12, 15, 16], and adequate spatial tuning is critical for distractor resistance. Whether the microcircuit components contributing to working memory in macaque dlPFC are present in marmoset dlPFC remains largely unknown. Marmosets have a smaller dlPFC than macaques[17-19], and marmoset prefrontal pyramidal neurons have fewer spines on the basal dendrites[20], which could be necessary for the recurrent excitation that supports persistent activity. Nevertheless, dlPFC delay-related persistent activity was recently verified in marmosets[21], suggesting they have the key microcircuit components to support working memory.

Neuromodulators such as dopamine (DA) have powerful effects on dlPFC function in macaques[22] and marmosets[23]. In macaques, this is largely mediated by D1Rs[22, 24], with an inverted-U dose-response, where mid-range levels of D1R stimulation facilitate working memory[25, 26], while higher levels impair working memory[27, 28]. In macaque dlPFC, D1Rs are prevalent on the dendritic spines of layer III pyramidal neurons[24, 26, 29], but they are also found on the dendrites of PV neurons[30]. *Ex vivo* physiological studies in rodents[31] and macaques[32] have shown that D1R stimulation increases the intrinsic excitability of fast-spiking, putative PV neurons, which could affect their role in sculpting the spatial tuning of excitatory Delay cells *in vivo*. A recent study using iontophoresis and electrophysiology in macaque dlPFC showed that DA, via D1Rs, modulates fast-spiking, likely PV neurons, during delay periods with distractor challenges[33]. Given the D1R-mediated increase in the excitability of fast-spiking, putative PV

neurons, which participate in shaping working memory processes during distractor challenges *in vivo*, we hypothesize that higher D1R expression levels in layer III dlPFC PV neurons in marmosets, compared to macaques, may significantly degrade working memory performance and specifically distractor resistance. Because these layer III microcircuits could be altered in schizophrenia[34], stage III/IV Alzheimer's disease[35], and stress and mood disorders[36], understanding their common and divergent properties across primates is critical when modeling neural mechanisms of cognitive disorders.

Here, we first compared the ability of marmosets and macaques to maintain gaze on a central point in the presence of visual distractors. Next, we assessed D1R expression in layer III dlPFC PV neurons across the two species by mining existing single-nucleus RNA sequencing (snRNA-seq) datasets and performing immunohistochemistry. Finally, we incorporated the anatomical measurements of D1R expression in a visuospatial working memory model to simulate the effect of higher D1R expression on inhibitory fast-spiking, putative PV neurons in a layer III dlPFC microcircuit. Our results demonstrate that marmosets exhibit more distractibility than macaques, even in a basic visual fixation task, and that marmosets have higher D1R expression in layer III dlPFC PV neurons. Lastly, our modeling shows that higher D1R expression in fast-spiking, putative PV neurons in a layer III dlPFC microcircuit may contribute to higher distractibility in marmosets by shifting the decreasing phase of the inverted-U response, characterized by distractibility, from the high to the typical, mid-range D1R stimulation levels. Our results suggest fundamental species differences in the effect of DA on dlPFC microcircuits and offer insights into mechanisms of distractibility in working memory.

Results

Marmosets are more distractible than macaques in a basic visual fixation task

To quantify differences in distractibility between marmosets and macaques, we used a basic fixation task with minimal cognitive demands. Specifically, we examined the ability of the species to hold visual fixation on a central point while distracting stimuli flashed in the visual periphery. This task is commonly used with rhesus macaques to map receptive field properties of neurons in visual cortical areas[37], and marmosets can perform it with a reasonable degree of success[38]. We analyzed data collected previously from eight marmosets and two macaques performing this task under comparable visual stimulation conditions[37, 38]. Animals were required to maintain fixation within a 1-2° radius around the fixation point while high contrast Gabor stimuli flashed at random positions in the periphery at 60 Hz. Monkeys were rewarded with a drop of juice for holding fixation at increasingly longer periods up to a maximum of 3 seconds.

The two macaques could ignore the distractors for over twice as long as any of the marmosets (Figure 1), holding fixation for a median duration of 2.57 seconds as compared to 1.05 seconds in marmosets, which was a significant cross-species difference (Ranksum test, $p=0.044$). Although individual marmoset performance varied considerably, no single marmoset achieved performance equivalent to either of the macaques (individuals shown with black circles, Figure 1). These data suggest that even when the cross-species comparison task has minimal cognitive demands, a fundamental difference in distractibility exists between the species.

Marmosets have higher DRD1 expression in dlPFC PVALB neurons than macaques

Analyses from two independent snRNA-seq datasets revealed that *DRD1* (the gene encoding D1R) expression in *PVALB* (the gene encoding PV) neuron clusters of the marmoset dlPFC is markedly higher than in macaque dlPFC (Figure 2). The first dataset compared expression in young adult marmosets[39] and macaques[40], and demonstrated higher expression of *DRD1* in *PVALB* clusters from marmoset than macaque (Figure 2A). The second dataset corroborated and extended these findings, demonstrating that *DRD1* expression in *PVALB* clusters of marmosets exceeded expression in macaques, and that marmoset dlPFC and mouse frontal cortex[41] exhibit high *DRD1* expression in *PVALB* clusters, (Figure 2B), whereas human dlPFC had the lowest expression, suggesting an inverse relationship with phylogenetic position.

Marmoset layer III dlPFC PV neurons have higher D1R expression than macaques

To examine the *in-situ* expression of D1R protein in layer III dlPFC, we labeled D1R and PV using immunohistochemistry (Figure 3A-B). In both species, strong D1R labeling was observed in the cytoplasmic and nuclear regions of PV neurons and putative pyramidal neurons, consistent with previous findings[30, 42, 43]. Labeling was also observed in pyramidal neuron apical dendrites, confirmed by co-labeling with the cytoskeletal protein microtubule-associated protein 2 (MAP2, Figure S1). In our PV-D1R labeled tissue, we sampled from layer III in both species using confocal microscopy. The sampling site images were analyzed in two independent ways: 1) using an automated higher throughput colocalization analysis of PV neuronal segments (Figure 3C-D), which computed the spatial extent to which PV+ processes contain colocalized PV+/D1R+ pixels; and 2) then using a manual analysis of D1R fluorescence intensity signal in PV somata (Figure 3G-H), to determine the proportion of neurons that were negative for D1R or expressed D1R weakly, moderately, or strongly.

For the colocalization analysis, we first used automatic segmentation to isolate PV neuronal processes. We then computed an index of colocalization, called the Manders' Overlap Coefficient (MOC), to determine the proportion of each PV segment that contained colocalized D1R+/PV+ pixels. Marmoset PV segments had a higher degree of colocalization with D1R than macaque PV segments (Fig. 3C). For both species, segmented particles found in the PV neuron soma and proximal dendrites had a higher degree of D1R colocalization than those in non-proximal dendrites (Figure 3D), and this disparity was greater in marmosets. The second analysis (schematized in Figure S2) binned PV neurons according to their level of D1R expression, and showed that macaques had slightly more D1R-negative PV neurons than marmosets (Figure 3E-H). The trend continued with marmosets having more D1R strongly labeled PV neurons than macaques (Figure 3H), though this was not significant.

Computational modeling of the effect of the species difference in D1R expression in layer III dlPFC PV neurons on distractibility

Given that D1R stimulation increases the intrinsic excitability of fast-spiking, putative PV neurons in macaque layer III dlPFC, and that PV neurons shape the spatial tuning of excitatory Delay cell activity, we investigated whether higher D1R expression in marmoset layer III dlPFC PV neurons may contribute to higher visuospatial distractibility. One possible mechanism for this could be by increasing the inhibition in the microcircuit within the typical, mid D1R stimulation range, which could suppress task-related persistent activity more strongly. For this purpose, we redesigned a classic spiking network model[44] of a visuospatial working memory microcircuit in macaque layer III dlPFC (Figure 4A1), which allows linking functional microanatomy with cognitive performance. Specifically, besides near feature-tuned excitatory (E) Delay cells (Figure 4A2), we incorporated two new fast-spiking inhibitory Delay cell types – I_{NEAR} and I_{OPP} – with near-feature and opposite-feature tuning (Figure 4A3-4A4), to replace the

unstructured inhibition in the original model, because evidence suggests that putative fast-spiking, PV neurons might mediate such structured inhibitory motifs instead in primary sensory[45-49] and higher-order association[50-52] cortex. Although both inhibitory cell types shape the spatial tuning of excitatory Delay cell activities, I_{NEAR}-mediated inhibition stabilizes the amplitude (i.e., max. firing rates), while I_{OPP}-mediated inhibition – the width, of the tuning curve[53]. Furthermore, in a decision-making microcircuit model[54], I_{NEAR}-mediated inhibition supports fine discrimination between representationally similar stimuli, while I_{OPP}-mediated inhibition supports the robust elimination of representationally dissimilar stimuli. Thus, the width of I_{OPP}-inhibition would determine the size of E cell sub-populations (i.e., the extent of the arc on the ring, which they occupy) that compete. Correspondingly, in visuospatial working memory tasks with distractors, we anticipate that I_{NEAR} cells may provide resistance to near distractors, while I_{OPP} cells may provide resistance to far distractors. Notably, since attentional processes share neuronal substrates with working memory[9, 10], the neurons supporting distractor resistance in our model should partly overlap with those involved in our visual fixation task. Thus, our simulations may identify a plausible neural mechanism for our behavioral measures of visuospatial distractibility.

D1R expression in E and I_{NEAR} cells facilitates the inverted-U response

We considered three cell type-specific D1R expression patterns, and explored which could reproduce the inverted-U relationship between D1R stimulation and persistent firing activity observed experimentally in delayed-response working memory tasks[24, 25, 27] (Figure 4B). Specifically, we built three networks in which E cells always expressed D1Rs, while D1R expression in the inhibitory cells differed. D1Rs were expressed in Network 1 by I_{NEAR} cells; in Network 2 by I_{OPP} cells; and in Network 3, by both I_{NEAR} and I_{OPP} cells. We considered D1R stimulation in terms of D1R occupancy, the fraction of DA-bound D1Rs. We defined five D1R occupancy levels – no (0), low (0.25), mid (0.50), high (0.75) and very high (1) – on a normalized scale ranging from 0 to 1, and evaluated network performance in a visuospatial working memory task. During task trials, we briefly presented a target stimulus at 0° and, later, a distractor stimulus at 180°, the most representationally dissimilar position. We varied the strength of stimuli to identify what strength evoked the most robust inverted-U response. Too weak stimuli will never elicit persistent activity, while too strong stimuli will always cause distractibility. To reproduce the distinct persistent activity regimes of the inverted-U for the macaque, we implemented a set of D1R modulations of synaptic and intracellular parameters, aiming to tune the signal-to-noise ratio[55] in the microcircuit. Specifically, we (1) increased the NMDAR conductance at E→E synapses[56, 57] ($G_{E\rightarrow E,\ NMDA}$) to facilitate a transition from a transient to a persistent activity regime and (2) decreased AMPAR conductances at E→E and E→I synapses[56, 58] ($G_{E\rightarrow E,\ AMPA}$, $G_{E\rightarrow I,\ AMPA}$) to dampen noise inputs to excitatory and inhibitory cells (Figure 4C1). Concurrently, we decreased the firing thresholds of D1R+ inhibitory cells to increase their intrinsic excitability (Figure 4C2). See details in Methods.

Network 1 reproduces the inverted-U over a range of stimulus strengths between ~0.15-0.30 pA with high reliability (max. fraction of complete inverted-Us of 99.1% at 0.20 pA) (Figure S4). Specifically, no and very high D1R occupancies result in transient activations in response to the stimuli due to, respectively, insufficient recurrent excitation and overinhibition (Figure 5A1 and 5E1). Low D1R occupancy elicits an overexcitable, erroneous regime, prone to spatially diffuse and noise-evoked persistent activity at non-stimulus positions (Figure 5B1). Mid D1R facilitates a spatially precise, noise- and distractor-resistant persistent activity regime, suggesting the network represents the memory more accurately during the delay period due to optimal inhibition (Figure 5C1). Notably, high D1R occupancy induces a distractible regime where persistent activity forms around the target position during the delay period but then jumps to the position of the distractor when it appears (Figure 5D1). In contrast, Network 2 cannot reproduce the

inverted-U (Figure S4), particularly the distractible persistent activity expected at high D1R occupancy. Network 3 reproduces the inverted-U, like Network 1, but over a narrower range between ~0.20-0.30 pA, and less reliably (max. fraction of complete inverted-Us of 67.7% at 0.25 pA) (Figure S4). Overall, microcircuits featuring D1R+ E and I_{NEAR} cells (Network 1 or 3) appear sufficient to reproduce the inverted-U relationship between D1R stimulation and *in-vivo* delay-period neuronal firing activity in visuospatial working memory tasks, unlike a microcircuit featuring only D1R+ E and I_{OPP} cells (Network 2). Our data suggest that D1R+ I_{NEAR} cells may represent D1R+ PV neurons because specifically D1R+ I_{NEAR} cells contributed, alongside D1R+ E cells, to the inverted-U response by increasing their intrinsic excitability with D1R stimulation, which occurs only for D1R+ fast-spiking, putative PV neurons[32]. This corroborates earlier[59, 60] and some more recent[61] indications that PV neurons provide near-feature inhibition in microcircuits.

Most plausible working memory performance in microcircuit with D1R+ I_{NEAR} and E cells, and D1R- I_{OPP} cells

To further evaluate the effect of inhibitory cell-type-specific D1R expression on the visuospatial working memory performance of Networks 1-3 (Figure S5), we simulated the effects of distractors presented at different positions. We focused on Networks 1 and 3, specifically at the typical, mid D1R occupancy level, because Network 2 cannot reproduce the inverted-U for distractors even at 180°. Whereas Network 3 performed poorly due to overwhelming distractibility or errors across distractor positions, with distractor resistance predominating only around 180°, Network 1 was overwhelmingly distractor-resistant at intermediate-to-far positions (112.5°-180°) but also significantly at near positions (45°). We also examined two alternative networks featuring E cells and only, respectively, I_{NEAR} or I_{OPP} cells (all D1R+) (Figure S6). The I_{NEAR}-only network exhibited significant resistance to near distractors (45°) but also overwhelming distractibility and errors across distractor positions. Conversely, the I_{OPP}-only network could overwhelmingly resist far distractors (112.5°-180°), while being highly distractible for near distractors (45°-90°). Furthermore, expectedly, the I_{OPP}-only network could not be distracted by far stimuli at high D1R occupancy (135°-180°). Overall, I_{NEAR} and I_{OPP} cells enable near and far distractor resistance, respectively, and both are necessary for effective microcircuit operations, with D1R expression in only E and I_{NEAR} cells (Network 1) enabling the most plausible performance. These results match experimental observations in a similar visuospatial working memory task[62], which suggested that macaque dlPFC microcircuitry provides some resistance to near distractors (45°) and strong resistance to far distractors (135°, 180°).

Distractibility induced at the typical, mid D1R occupancy level in marmoset

To examine how the higher D1R expression in layer III PV neurons from marmoset dlPFC could affect distractibility in marmosets, we integrated our anatomical findings into the most plausible Network 1. Specifically, given the cross-species difference in D1R expression in PV neurons (Figure 3), and since D1R+ I_{NEAR} cells likely represent D1R+ PV neurons, we assumed that more D1Rs will be DA-bound on I_{NEAR} cells in marmoset compared to macaque, provided there is similar extracellular DA concentration in dlPFC across conditions between both species. Essentially, the same D1R occupancy signifies greater D1R stimulation of marmoset dlPFC PV neurons. Thus, we shifted the midpoint of the I_{NEAR} threshold sigmoid from the reference value of 0.50 for the macaque, on the normalized D1R occupancy scale, to 0.36 for the marmoset, based on the difference (0.14) in mean MOCs between the species (Figure 4C2).

As in the macaque, the marmoset shows only transient activity for no and very high D1R occupancy (Figure 5A2 and 5E2). For low D1R occupancy, the marmoset overwhelmingly exhibits erroneous spatially diffuse, noise-driven persistent activity (Figure 5B2), but with a lower frequency of 85.4% compared to the macaque's 97.3% (Figure S7A-S7B). Crucially, for mid D1R occupancy (Figure 5C2), the marmoset demonstrates distractible persistent activity, which can be verified experimentally, with a frequency of 87.2%, unlike the macaque's 99.7% distractor-resistant persistent activity (Figure S7A-S7B). Finally, at high D1R occupancy, the marmoset already transitions to the transient activity regime (Figure 5D2), which occurs at a higher D1R occupancy in the macaque (Figure S7A-S7B). Overall, the model predicts that the higher D1R expression in I_{NEAR} cells (putative D1R+ PV neurons) in marmoset layer III dlPFC shifts the apex and decreasing phase of the inverted-U to lower D1R occupancy levels for the marmoset, compared to the macaque, since the optimal I_{NEAR}-mediated inhibition is closer to the peak NMDAR-mediated excitation. Thus, the typical, mid D1R occupancy range supports spatially precise, noise- and distractor-resistant persistent activity in macaques, while inducing distractible persistent activity in marmosets.

However, because differences in MOC-measured D1R expression may not correspond directly to differences in D1R stimulation, we examined larger sigmoid midpoint shifts (Figure S7C-S7D). Notably, a shift of 0.375 was approximately the largest that still supports (distractible) persistent activity at the typical, mid D1R occupancy in the marmoset before the microcircuit enters a transient activity regime. Thus, shifts between approx. 0.14-0.375 would capture the cross-species differences in distractibility, while allowing for plausible microcircuit functioning in the typical, mid D1R stimulation range.

Discussion:

We have shown that marmosets are more distractible than macaques, even in a basic visual fixation task. Furthermore, we found lower *DRD1* expression in *PVALB* neurons in marmosets, compared to macaques, which may constitute a phylogenetic trend, and we confirmed *in situ* that layer III dlPFC PV neurons have higher D1R expression in marmosets. Finally, our microcircuit model suggests that higher D1R expression in fast-spiking, putative PV neurons (as we observed in marmosets) shifts the distractible persistent activity regime of the inverted-U response leftward, such that the typical, mid levels of D1R occupancy may cause more distractible behavior. To our knowledge, this is the first study to examine how D1R expression differences in PV neurons may affect a cognitively engaged, non-human primate dlPFC microcircuit. Notably, causal manipulations of *in vivo* D1R expression in PV neurons are not possible in non-human primates with current technology.

Longstanding electrophysiological and behavioral evidence in marmosets and macaques has implicated DA in working memory and distractor resistance[22, 23, 63-65], but specific microcircuit mechanisms remain an active research area. D1R prevalence on the dendritic spines of dlPFC pyramidal neurons positions them to enhance NMDAR actions in the synapse and, thus, strengthen recurrent excitation to facilitate distractor-resistant persistent activity in Delay cell networks[24, 62, 66]. D1Rs may further reduce weak signals and ensure appropriate tuning by shunting network inputs via the opening of K+ channels on some spines[24, 28, 67]. Alternatively, D1R stimulation may also affect distractor resistance by modulating cortical inhibition[57, 68, 69]. In rodents and macaques, D1Rs have been shown to increase inhibition through fast-spiking[31, 32, 58], non-fast spiking[70], or vasoactive intestinal peptide-expressing (VIP) inhibitory neurons[71]. However, we modeled DA modulation of inhibition strictly based on the evidence in macaque layer III dlPFC that D1Rs excite fast-spiking, putative PV neurons[32].

Our results suggest that the effect of D1R-mediated modulation of inhibition on working memory performance depends on whether inhibitory neurons target other neurons tuned to near or opposite features of stimulus space with their highest inhibitory strength[53]. Previous spiking network models of dlPFC microcircuits have featured unstructured[44, 72] or structured [73] I_{NEAR}-mediated inhibition. However, while near and opposite feature-tuned inhibitory neurons have both been studied[16, 49-52, 74], few models of association cortex have incorporated I_{OPP}-mediated inhibition[52-54, 75], and, to our knowledge, no studies have investigated how D1R modulation of either inhibitory cell type affects cognition, especially in a continuous attractor network. Therefore, we modeled I_{NEAR} and I_{OPP} cells, and explored how inhibitory cell-type-specific D1R modulation may enable the microcircuit to reproduce the inverted-U response observed in macaques *in vivo*. We found that a microcircuit that features excitatory and both inhibitory Delay cell types, and where D1Rs modulate E cells and I_{NEAR} cells (putative D1R+ PV neurons), can capture D1R effects on persistent activity and reproduce the distractor distance-dependent pattern of working memory performance seen in macaques[62]. Hence, optimal D1R stimulation may facilitate primarily the stabilization of the amplitude, and not of the spatial extent, of tuned excitatory Delay cell activity[14].

By integrating our anatomical results into our most plausible network configuration, we propose that differential D1R modulation of layer III dlPFC PV neurons may underlie cognitive differences between marmosets and macaques. Specifically, the higher D1R expression in layer III dlPFC PV neurons in marmosets may contribute to their higher distractibility by shifting the distractible persistent activity regime of the inverted-U response to the typical, mid D1R occupancy range. Conversely, the same level of DA stimulation in macaques supports appropriately tuned and distractor-resistant persistent activity for visuospatial working memory performance. Interestingly, the D1R occupancy range that induces erroneous persistent activity in the increasing phase of the inverted-U contracted for the marmoset in our modelling, predicting that this species is less susceptible to internal distractions (context-irrelevant mental representations, formed without sensory input, that overtake network dynamics). Notably, however, the model assumes extracellular DA concentration in dlPFC is similar across neurophysiological or environmental conditions between the species, and hence mid D1R occupancy is the level at which they both function normally. To our knowledge, no studies have demonstrated species differences in DA innervation of dlPFC. However, DA release could vary significantly over time for marmosets and macaques, and thus both species may utilize the entire D1R occupancy scale more frequently, instead of primarily functioning within the mid D1R occupancy range. In that scenario, a reduced range of D1R occupancies that support distractor-resistant persistent activity in marmosets (e.g., Figure S7C) could better explain their higher distractibility. Otherwise, the fewer spines on the basal dendrites of pyramidal neurons, potentially leading to weaker recurrent excitation, in marmoset dlPFC[20] could also significantly contribute to the higher distractibility. In our model, decreasing the maximum strength of E→E synapses for the marmoset would account for this species difference. In effect, this would cap recurrent excitation to a lower level, and the D1R-mediated increase of $G_{E\rightarrow E,\,NMDA}$ would not facilitate the same amplitude of persistent activity as in the macaque, decreasing the distractor resistance of the microcircuit.

Importantly, a recent model suggested that D1R modulation of somatostatin (SST; similar to calbindin (CB) in primates) and VIP (similar to calretinin (CR) in primates) inhibitory neurons also affect working memory performance[69]. The I_{OPP} cells in our study may represent D1R-/PV+ neurons, perhaps about a third of the total layer III dlPFC PV population according to our manual anatomical analysis (Figure 3H). Alternately, SST/CB neurons have been implicated in opposite feature-tuned inhibition[52, 69, 76, 77] and can display fast spikes, like PV neurons[78, 79] and the inhibitory cells in our model. Since CB neurons target the distal dendritic trees of pyramidal neurons[80], theoretical studies[69, 76] have suggested they could dampen

inputs into the distal dendrites and thus attenuate the effect of noise or distracting stimuli on network dynamics. However, the identities of distal dendrite inputs are unclear and are likely not all task-irrelevant. Moreover, both I_{NEAR} and I_{OPP} cells in our model synapse on the E-cell soma because our E cells lack dendritic compartments, questioning a clear correspondence between I_{OPP} cells and SST/CB neurons, and supporting a correspondence with perisomatic PV neurons. Finally, our model lacks disinhibitory VIP/CR neurons, which perform permissive gating for pertinent incoming signals[76, 80-82]. The CR neuron population has expanded in primates[83], and CR neurons are more prominent in the dlPFC compared to earlier parts of the dorsal stream[78], suggesting a critical role in higher cognition. Future studies should explore species differences in D1R modulation of CB and CR neurons, which are also critical components of cortical microcircuits.

The current findings suggest that there may also be species differences in DA modulation during stress exposure, when DA release in dlPFC rapidly increases[28, 84, 85]. Excessive D1R stimulation eventually silences excitatory Delay cell activity, which may be a mechanism for diverting energy resources from cognitive processes to survival processes that support the navigation of stressful circumstances and threats[27, 28, 86-89]. Overstimulation of D1Rs in PV neurons may contribute to this process by increasing the level of perisomatic inhibition on isotuned excitatory Delay cells, thus suppressing persistent activity that could otherwise be appropriately tuned for attention or working memory. Our model suggests that this could occur more rapidly for marmosets during rising DA release. Although faster D1R-mediated PV suppression of dlPFC activity may limit behavioral flexibility in states of stress, the resulting higher susceptibility of cognitive processes to interference by external stimuli may benefit survival in smaller prey species like marmosets by lowering the threshold for predator detection. Conversely, the lower susceptibility to interference by external stimuli in macaques may be indicative of an expanded top-down processing capacity and, thus, greater behavioral flexibility in states of stress. Our inter-species sequencing data suggest that these inferences could extend to mice and humans.

To conclude, our multi-scale study explored behavioral correlates of cognitive function, *DRD1* mRNA and D1R protein levels *in situ*, and computational modeling of molecular, cellular, and microcircuit bases of working memory performance. Our findings indicate a general mechanism by which subtle cell type-specific molecular differences in dlPFC microcircuits may significantly affect cognitive function. Specifically, we found that a difference in the expression of one receptor in one cell type, namely D1R in layer III dlPFC PV neurons, may contribute to species differences in distractibility, even in tasks with minimal cognitive demands. Notably, we empirically confirm marmosets are more distractible than macaques – a crucial step in understanding the viability of the former as animal models of cognition, and a note of caution about their translational validity. Furthermore, our results suggest that natural variation in D1R expression in PV neurons in humans may contribute to variation in distractibility. Finally, as working memory deficits and distractibility are key symptoms of schizophrenia and ADHD, differences in D1R expression in PV neurons in these psychiatric disorders are worth investigating.

Figure 1

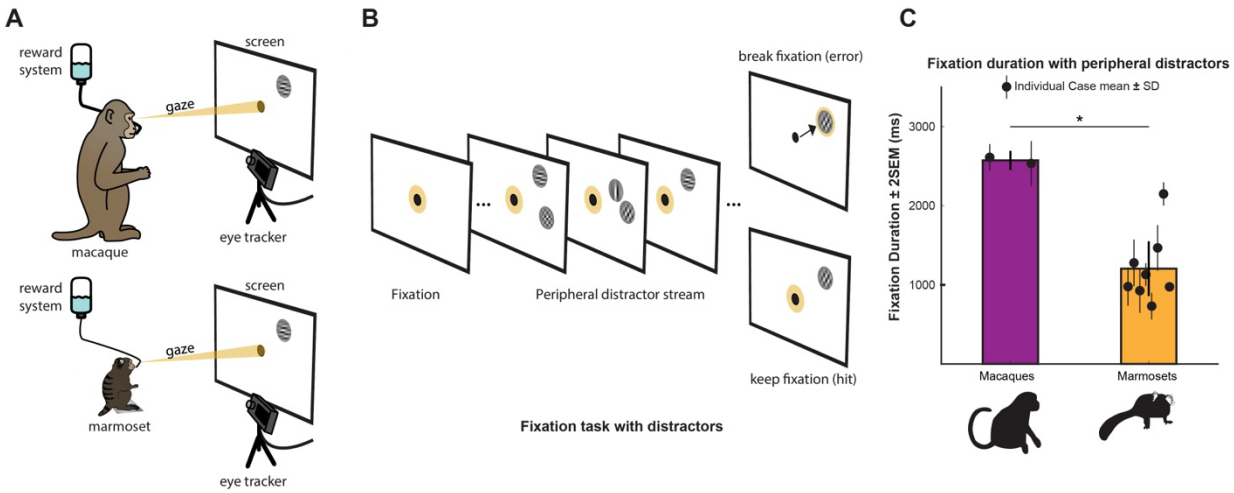

Figure 1 – Macaques held central fixation in the presence of peripheral distractors more than twice as long as marmosets. ***A,*** Schematic of the task setup. A macaque (top) and a marmoset (bottom) face a screen, and an eye tracker monitors their eye movements. Monkeys receive a juice reward for maintaining fixation at the central point in the presence of peripheral distractors. ***B,*** Schematic of the task progression. A point appears at the center of the screen, and the monkey fixes its gaze (yellow) on the central point. Gabor stimuli flash in and out of the periphery, and the monkey is rewarded for maintaining its fixation on the central target ("hit") despite the distracting peripheral stimuli. ***C,*** Time held fixating at a central point in the presence of visual distractors across species. Bars indicate group mean fixation duration for two macaques (purple) and for eight marmosets (orange). Thick black lines depict ± 2 standard error of the mean (SEM); Black circles and thin lines depict individual subject mean fixation duration ± standard deviation (SD). *, $p < 0.05$, Ranksum test.

Figure 2

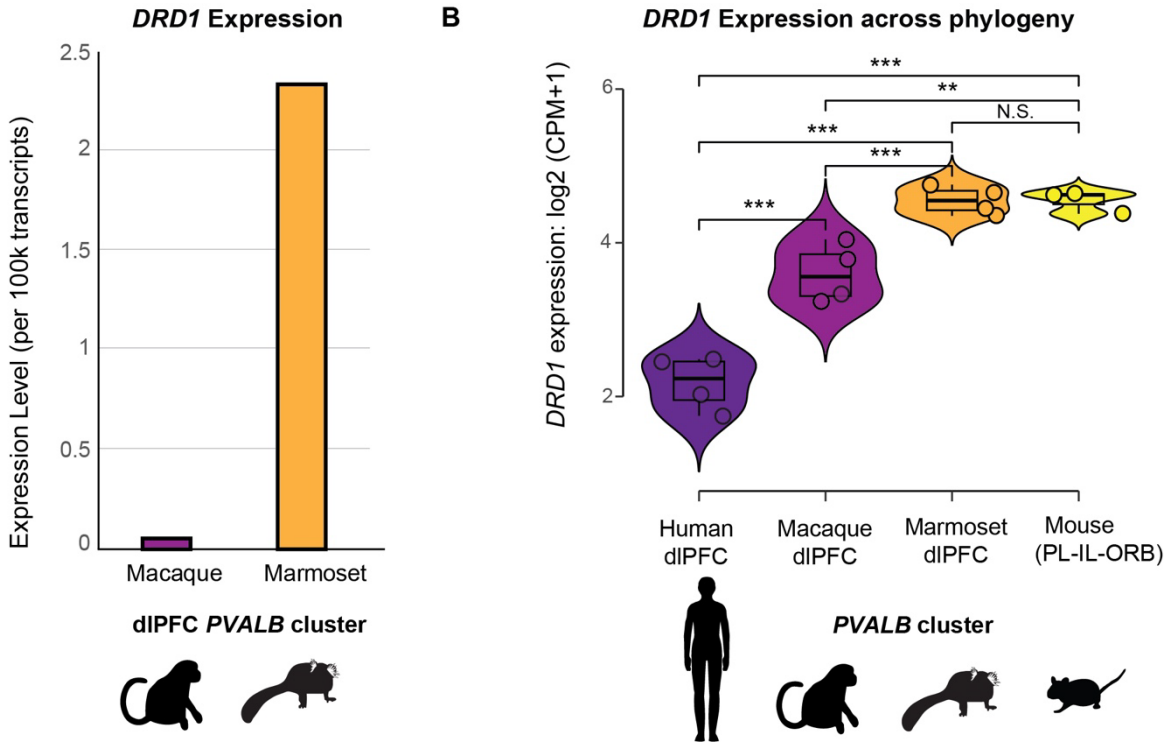

Figure 2 – Marmoset dlPFC *PVALB* neurons have higher *DRD1* expression than macaque *PVALB* neurons. ***A,*** *DRD1* expression in *PVALB* clusters of the dlPFC in macaques (purple) and marmosets (orange), depicted as expression per 100,000 transcripts. ***B,*** Library size-normalized expression of *DRD1* in adult cortical *PVALB* neurons across human dlPFC (dark purple), macaque dlPFC (plum), marmoset dlPFC (orange), and mouse frontal cortex (yellow). Data mined from Ma *et al*.[90]. Due to the lack of dlPFC homology in mice, we included mouse PL-IL-ORB (prelimbic, infralimbic and orbital regions, yellow) regions from Yao et al.[41], which are analogous substrates for some primate dlPFC cognitive functions. Each dot represents a pseudobulk donor and the significance of the gene expression differences was tested by edgeR[91]. CPM, counts per million; ***, $P < 0.001$; **, $P < 0.01$; N.S., not significant.

Figure 3

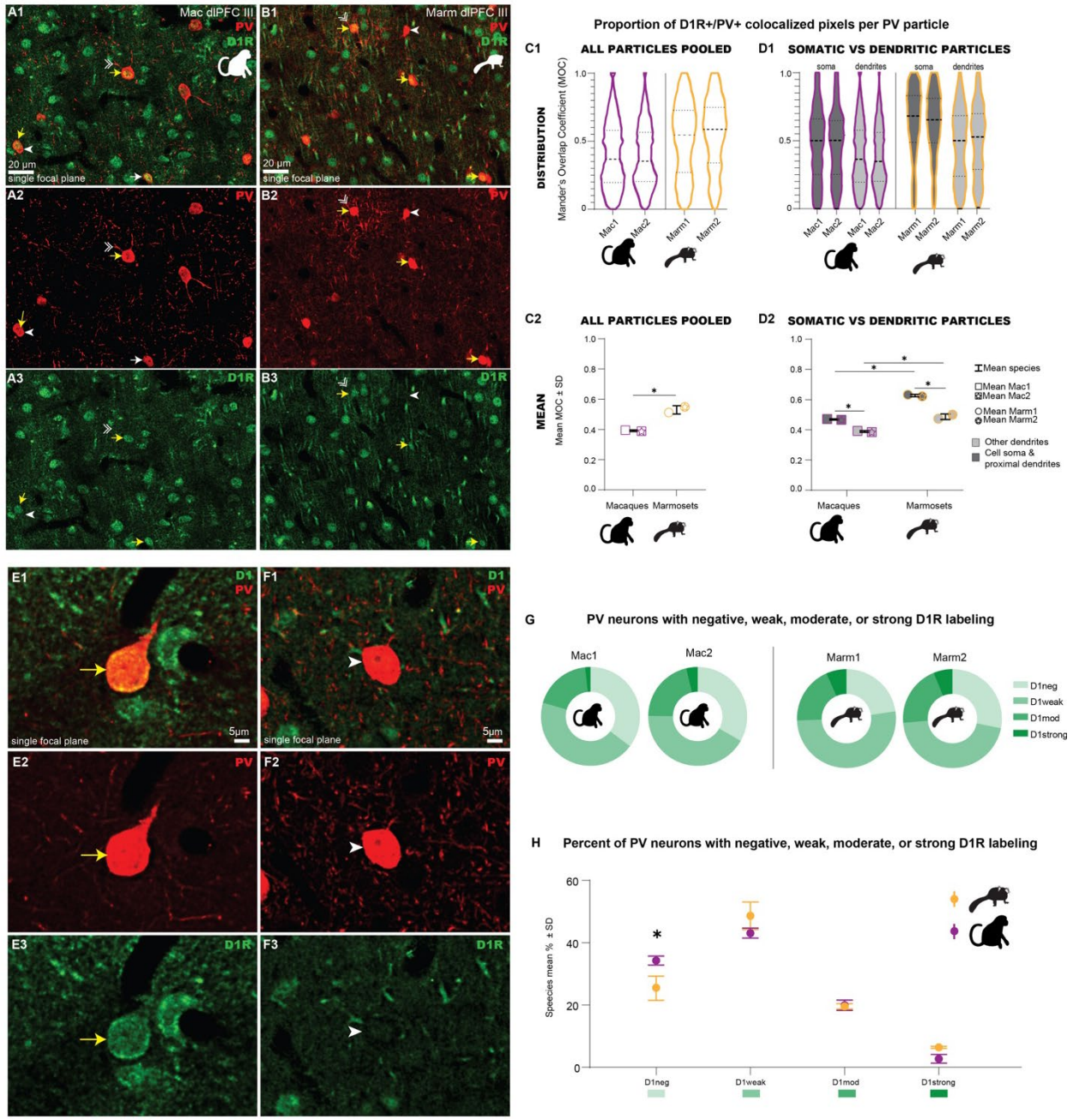
A1
Mac dlPFC III
PV
D1R
20 µm
single focal plane
B1
Marm dlPFC III
A2
B2
A3
B3
E1
D1
PV
F1
5µm
E2
F2
E3
F3
Proportion of D1R+/PV+ colocalized pixels per PV particle
C1
ALL PARTICLES POOLED
D1
SOMATIC VS DENDRITIC PARTICLES
DISTRIBUTION
Mander's Overlap Coefficient (MOC)
soma
dendrites
Mac1
Mac2
Marm1
Marm2
C2
ALL PARTICLES POOLED
D2
SOMATIC VS DENDRITIC PARTICLES
MEAN
Mean MOC ± SD
Macaques
Marmosets
Mean species
Mean Mac1
Mean Mac2
Mean Marm1
Mean Marm2
Other dendrites
Cell soma & proximal dendrites
G
PV neurons with negative, weak, moderate, or strong D1R labeling
D1neg
D1weak
D1mod
D1strong
H
Percent of PV neurons with negative, weak, moderate, or strong D1R labeling
Speecies mean % ± SD

Figure 3 – Marmosets have higher correlates of D1R protein expression in layer III dlPFC PV neurons than macaques. ***A-B,*** Confocal photomicrographs with brightness and contrast adjustments depicting a single focal plane imaged in layer III of the macaque **(A)** and marmoset **(B)** dlPFC labeled for PV (red) and D1R (green)**.** Images depict some PV neurons robustly expressing D1R (yellow arrows), or not expressing D1R (white arrowhead). Double-headed white arrow heads depict proximal PV dendrites, defined by being traceable to a parent PV soma. ***C1,*** Violin plots with medians and quartiles, depicting kernel density of the MOC pooled across all PV particles by subject. MOC roughly measures the proportion of D1R+/PV+ pixels in each PV particle. Macaques, purple; marmosets, orange. ***C2,*** Species MOC means for all PV particles (marmosets MOC 0.53±0.03, macaque 0.39±0.01; two-tailed t-test, t(2)=7.283, p=0.0183). ***D1,*** Violin plots with medians and quartiles, depicting kernel density of the MOC across subjects for PV particles segregated into two categories: somata + proximal dendrites, dark grey; or other dendrites not traceable to a soma, light grey. ***D2,*** MOC means across species and proximity to soma classification [mean MOC marmosets soma and proximal, 0.62±0.01; marmoset other 0.47±0.02; macaque soma and proximal 0.47±0.004, macaque other 0.39±0.01; two-way ANOVA, species two-way ANOVA; $F_{1,4}$ = 293.7, p<0.0001; proximity to soma $F_{1,4}$ = 216.9, p=0.0001; interaction $F_{1,4}$ = 16.27, p=0.0157; Pairwise testing with Sidak's multiple comparisons corrections confirmed significant effects within species (marm prox vs. marm other p=0.0011; macaque prox vs. macaque other, p=0.0098), and between species (marm prox vs. macaque prox, p=0.0007; marm other vs. macaque other, p=0.0045)]. ***E-F,*** Confocal photomicrographs of single focal planes imaged in layer III dlPFC labeled for PV (red) and D1R (green). Images depict exemplar PV neurons that fell in the D1R strong category (yellow arrows, E), or D1R negative category (white arrowheads, **F**) for analyses in ***G-H***. ***G,*** Proportion of PV neurons falling into four D1R expression bins by subject. Bins were determined objectively for each individual image by binning the image's own D1R signal intensity range. To be classified as D1neg, D1R mean grey value (MGV) in the PV neuron was less than the average D1R MGV sampled in the immunonegative "neuropil". To be classified as D1strong, the D1R MGV of the PV neuron was above the minimum MGV of the most "strongly" labeled D1R neurons in the image, which were typically pyramidal in morphology. Intermediate categories D1weak and D1moderate are intermediate bins between D1neg and D1strong. ***H,*** Species mean for each D1R expression category (mean D1neg marmosets 25±4%, macaques 35±1%, two-way ANOVA, F (3.8) = 215.4, p<0.001, with Sidak's pairwise multiple comparison test, p=0.0221; mean D1neg marmosets 6±0.3%, macaques 3±1%, n.s.). Macaques, purple; marmosets, orange. *, p <0.05 using two-way ANOVA with Sidak's post-hoc pairwise comparisons; D1R, dopamine 1 receptor; dlPFC, dorsolateral prefrontal cortex; Mac, macaque; Marm, marmoset; MOC, Manders' Colocalization Coefficient; PV, parvalbumin; SD, standard deviation.

Figure 4

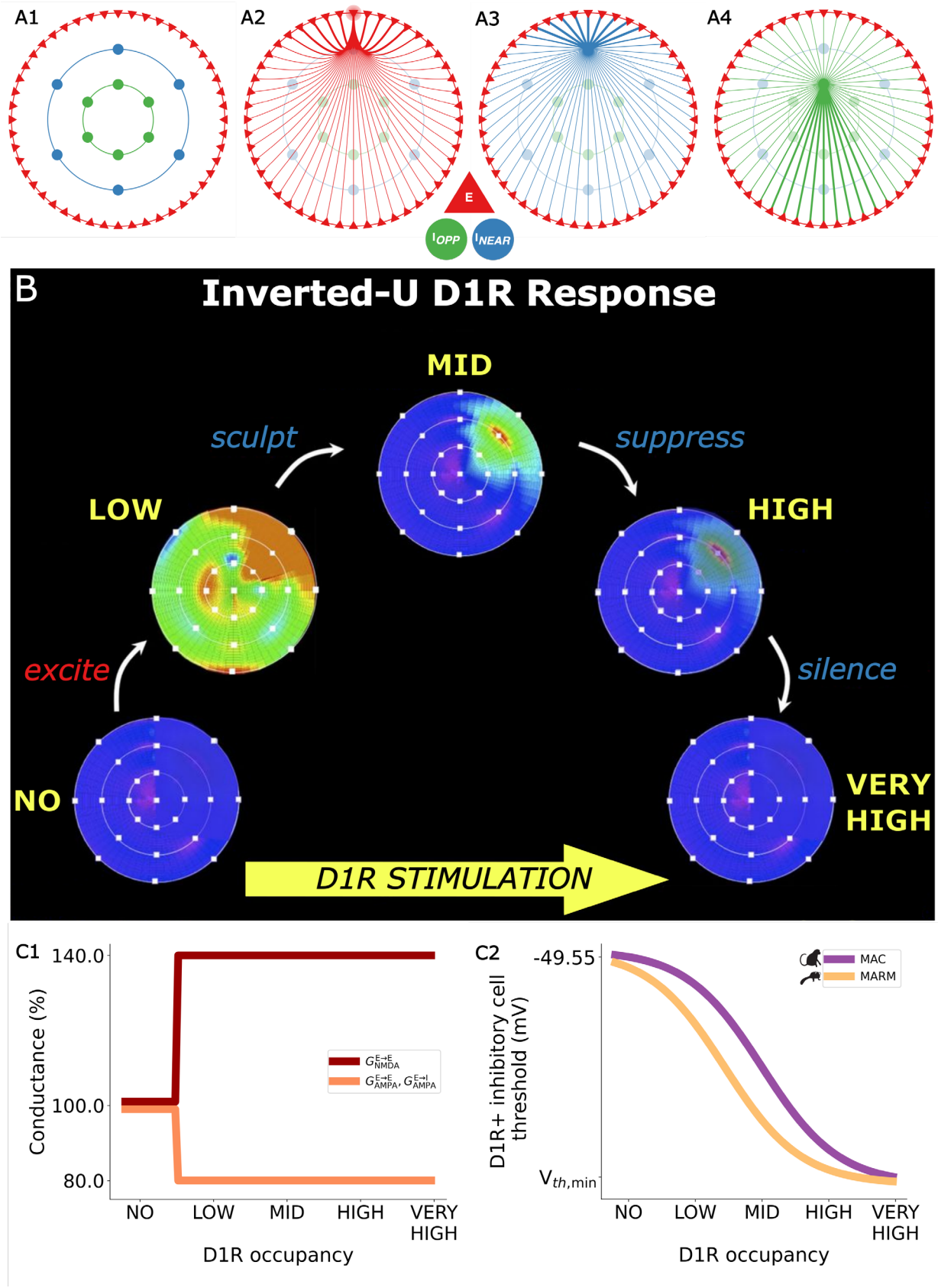
A1
A2
A3
A4
E
I OPP
I NEAR
B
Inverted-U D1R Response
MID
sculpt
suppress
LOW
HIGH
excite
silence
NO
VERY HIGH
D1R STIMULATION
C1
140.0
100.0
80.0
Conductance (%)
NO
LOW
MID
HIGH
VERY HIGH
D1R occupancy
C2
-49.55
D1R+ inhibitory cell threshold (mV)
MAC
MARM
NO
LOW
MID
HIGH
VERY HIGH
D1R occupancy

Figure 4 – Spiking neural network architecture and synaptic connectivity, the inverted-U relationship between D1R stimulation and persistent activity during the delay period of visuospatial working memory tasks, and microcircuit effects of D1R occupancy. ***A***, Simplified schematic representations of **(A1)** the ring architecture of the network comprising 80% near feature-tuned E cells, 10% I_{NEAR} cells, and 10% I_{OPP} cells, with example connectivity profiles for **(A2)** an E cell to each other E cell, **(A3)** an I_{NEAR} cell to all E cells, and **(A4)** an I_{OPP} cell to all E cells, where the source cell is positioned at 0°. For each profile, a halo surrounds the cell from which the projections originate. Projection thickness indicates relative connection strength. E cells are arranged uniformly on a ring, in feature space, according to the angle of the visual stimuli for which they fire the most. Inhibitory cells are also arranged uniformly, based on the angular position of the E cells from which they receive the strongest excitation. The microcircuit features E→E, E→I, I→E, and I→I synapses. E cells send their strongest glutamatergic projections to all cells at the same angle as themselves. I_{NEAR} cells send their strongest GABAergic projections to all cells also at the same angle as themselves, while I_{OPP} cells – to all cells positioned 180° away from them on the ring. ***B,*** Diagram illustrating the idealized inverted-U response, characterized by the delay-period activity during visuospatial working memory tasks in macaques under varying D1R stimulation conditions (adapted with permission from Arnsten *et al.*[24]). At one extreme, no D1R stimulation means E cells cannot sustain persistent activity during the delay period, with only transient activity recorded during stimulus presentation. In the increasing phase of the inverted-U, low (suboptimal) D1R stimulation induces erroneous (noise-evoked and/or spatially diffuse) persistent activity due to overexcitation. At the peak of the inverted-U, mid (optimal) D1R stimulation sculpts spatially precise, noise- and distractor-resistant persistent activity. Crucially, at the decreasing phase of the inverted-U, high (supraoptimal) D1R stimulation suppresses E cells, decreasing their firing rates, and thus increasing the susceptibility of the persistent activity for target stimuli to disruptions by distractors. Finally, at the other extreme of the inverted-U, very high D1R stimulation silences E cells completely, precluding the formation of persistent activity, again with only transient activity being recorded during stimulus presentation. ***C1,*** Step-like relationships between D1R occupancy and (1) $G_{E\rightarrow E,\ NMDA}$ and (2) $G_{E\rightarrow E,\ AMPA}$ and $G_{E\rightarrow I,\ AMPA}$, as percentages of their respective baseline values. From no to low D1R occupancy, specifically at $x = 0.125$, we increased $G_{E\rightarrow E,\ NMDA}$ by 40% and decreased $G_{E\rightarrow E,\ AMPA}$ and $G_{E\rightarrow I,\ AMPA}$ by 20%. We applied the same D1R modulations of $G_{E\rightarrow E,\ NMDA}$, $G_{E\rightarrow E,\ AMPA}$, and $G_{E\rightarrow I,\ AMPA}$, in the marmoset and the macaque. ***C2,*** Sigmoidal relationship between D1R occupancy and the species-specific firing thresholds of the D1R+ inhibitory cells across networks. We decreased the firing thresholds of D1R+ inhibitory cells from their baseline ($V_{th,\ base}$) of -49.55 mV at no D1R occupancy, through the low, mid, and high levels, and to a minimum ($V_{th,\ min}$) at the very high level. $V_{th,\ min}$ differs across networks, as listed in Table 4 in Methods.

Figure 5

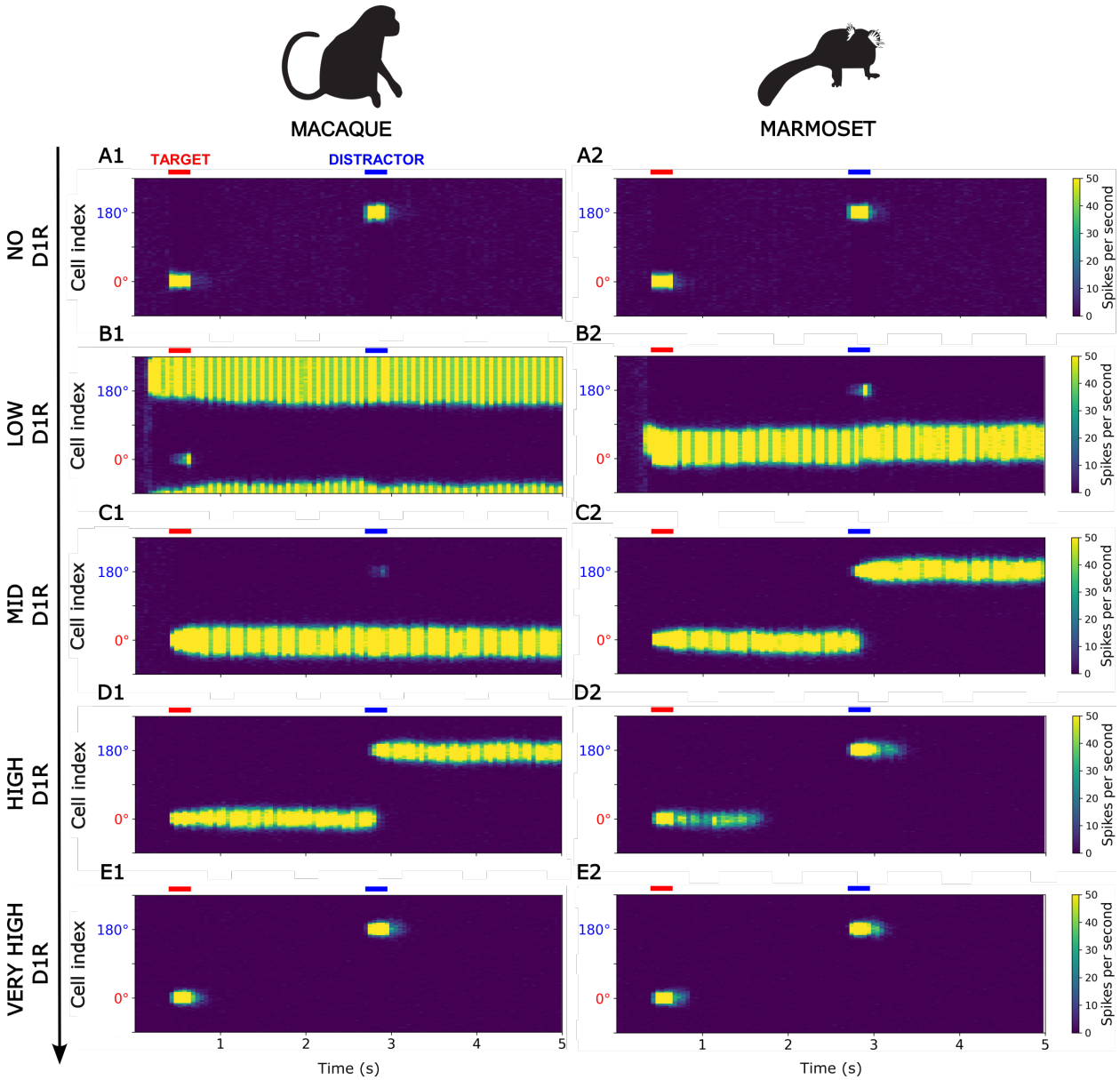

Figure 5 – Distractible, decreasing phase of inverted-U shifted to typical, mid D1R occupancy in the marmoset. Rastergrams represent the colour-coded, unmanipulated spike time series for macaque **(A1-E1)** and marmoset **(A2-E2)** of E cells in Network 1, during example five-second trials of the simulated visuospatial working memory task across the five D1R occupancy levels **(A-E)**. E cells are indexed by the angular position from 0° to 360° of their preferred stimulus. The strength of the stimuli is 0.20 pA. For visualization purposes, the y-axis wraps around 270° to accentuate the target (0°) and distractor (180°) positions, and the colour scale is capped to reduce the dominance of outliers in the heatmap, such that any firing rate of >50 Hz per second per neuron is plotted in the same colour as firing rates of 50 Hz.

References

1. Kumita, W., *et al.* Efficient generation of Knock-in/Knock-out marmoset embryo via CRISPR/Cas9 gene editing. *Scientific reports* **9**, 12719 (2019).
2. Oikonomidis, L., *et al.* A dimensional approach to modeling symptoms of neuropsychiatric disorders in the marmoset monkey. *Developmental neurobiology* **77**, 328-353 (2017).
3. Glavis-Bloom, C., Vanderlip, C.R. & Reynolds, J.H. Age-Related Learning and Working Memory Impairment in the Common Marmoset. *J Neurosci* **42**, 8870-8880 (2022).
4. Nakamura, K., *et al.* A Method to Train Marmosets in Visual Working Memory Task and Their Performance. *Frontiers in behavioral neuroscience* **12**, 46 (2018).
5. Miles, R.C. Delayed-response learning in the marmoset and the macaque. *J Comp Physiol Psychol* **50**, 352-355 (1957).
6. Weed, M.R., Bryant, R. & Perry, S. Cognitive development in macaques: attentional set-shifting in juvenile and adult rhesus monkeys. *Neuroscience* **157**, 22-28 (2008).
7. Clarke, H.F., *et al.* Prefrontal serotonin depletion affects reversal learning but not attentional set shifting. *J Neurosci* **25**, 532-538 (2005).
8. Prins, N.W., *et al.* Common marmoset (Callithrix jacchus) as a primate model for behavioral neuroscience studies. *J Neurosci Methods* **284**, 35-46 (2017).
9. Panichello, M.F. & Buschman, T.J. Shared mechanisms underlie the control of working memory and attention. *Nature* **592**, 601-605 (2021).
10. Mendoza-Halliday, D. & Martinez-Trujillo, J.C. Neuronal population coding of perceived and memorized visual features in the lateral prefrontal cortex. *Nature communications* **8**, 15471 (2017).
11. Mendoza-Halliday, D., Xu, H., Azevedo, F.A.C. & Desimone, R. Dissociable neuronal substrates of visual feature attention and working memory. *Neuron* **112**, 850-863.e856 (2024).
12. Goldman-Rakic, P.S. Cellular basis of working memory. *Neuron* **14**, 477-485 (1995).
13. Arnsten, A.F. The neurobiology of thought: the groundbreaking discoveries of Patricia Goldman-Rakic 1937-2003. *Cereb Cortex* **23**, 2269-2281 (2013).
14. Tanaka, S. Computational approaches to the architecture and operations of the prefrontal cortical circuit for working memory. *Progress in Neuro-Psychopharmacology and Biological Psychiatry* **25**, 259-281 (2001).
15. Roussy, M., *et al.* Ketamine disrupts naturalistic coding of working memory in primate lateral prefrontal cortex networks. *Mol Psychiatry* **26**, 6688-6703 (2021).
16. Rao, S.G., Williams, G.V. & Goldman-Rakic, P.S. Destruction and creation of spatial tuning by disinhibition: GABA(A) blockade of prefrontal cortical neurons engaged by working memory. *J Neurosci* **20**, 485-494 (2000).
17. Chaplin, T.A., Yu, H.H., Soares, J.G., Gattass, R. & Rosa, M.G. A conserved pattern of differential expansion of cortical areas in simian primates. *J Neurosci* **33**, 15120-15125 (2013).
18. Burman, K.J., Palmer, S.M., Gamberini, M. & Rosa, M.G. Cytoarchitectonic subdivisions of the dorsolateral frontal cortex of the marmoset monkey (Callithrix jacchus), and their projections to dorsal visual areas. *J Comp Neurol* **495**, 149-172 (2006).
19. Kaas, J.H. Comparative Functional Anatomy of Marmoset Brains. *ILAR J* **61**, 260-273 (2020).
20. Elston, G.N., *et al.* Specializations of the granular prefrontal cortex of primates: implications for cognitive processing. *The anatomical record. Part A, Discoveries in molecular, cellular, and evolutionary biology* **288**, 26-35 (2006).
21. Wong, R.K., Selvanayagam, J., Johnston, K.D. & Everling, S. Delay-related activity in marmoset prefrontal cortex. *Cereb Cortex* **33**, 3523-3537 (2023).
22. Vijayraghavan, S., Major, A.J. & Everling, S. Neuromodulation of Prefrontal Cortex in Non-Human Primates by Dopaminergic Receptors during Rule-Guided Flexible Behavior and Cognitive Control. *Front Neural Circuits* **11**, 91 (2017).
23. Crofts, H.S., *et al.* Differential effects of 6-OHDA lesions of the frontal cortex and caudate nucleus on the ability to acquire an attentional set. *Cereb Cortex* **11**, 1015-1026 (2001).

24. Arnsten, A.F., Wang, M. & Paspalas, C.D. Dopamine's Actions in Primate Prefrontal Cortex: Challenges for Treating Cognitive Disorders. *Pharmacol Rev* **67**, 681-696 (2015).
25. Williams, G.V. & Goldman-Rakic, P.S. Modulation of memory fields by dopamine D1 receptors in prefrontal cortex. *Nature* **376**, 572-575 (1995).
26. Wang, M.*, et al.* A novel dopamine D1 receptor agonist excites delay-dependent working memory-related neuronal firing in primate dorsolateral prefrontal cortex. *Neuropharmacology* **150**, 46-58 (2019).
27. Vijayraghavan, S., Wang, M., Birnbaum, S.G., Williams, G.V. & Arnsten, A.F. Inverted-U dopamine D1 receptor actions on prefrontal neurons engaged in working memory. *Nat Neurosci* **10**, 376-384 (2007).
28. Gamo, N.J.*, et al.* Stress Impairs Prefrontal Cortical Function via D1 Dopamine Receptor Interactions With Hyperpolarization-Activated Cyclic Nucleotide-Gated Channels. *Biol Psychiatry* **78**, 860-870 (2015).
29. Bergson, C.*, et al.* Regional, cellular, and subcellular variations in the distribution of D 1 and D 5 dopamine receptors in primate brain. *J Neurosci* **15**, 7821-7836 (1995).
30. Glausier, J.R., Khan, Z.U. & Muly, E.C. Dopamine D1 and D5 receptors are localized to discrete populations of interneurons in primate prefrontal cortex. *Cereb Cortex* **19**, 1820-1834 (2009).
31. Seamans, J.K., Gorelova, N., Durstewitz, D. & Yang, C.R. Bidirectional dopamine modulation of GABAergic inhibition in prefrontal cortical pyramidal neurons. *J Neurosci* **21**, 3628-3638 (2001).
32. Kröner, S., Krimer, L.S., Lewis, D.A. & Barrionuevo, G. Dopamine increases inhibition in the monkey dorsolateral prefrontal cortex through cell type-specific modulation of interneurons. *Cereb Cortex* **17**, 1020-1032 (2007).
33. Jacob, S.N., Stalter, M. & Nieder, A. Cell-type-specific modulation of targets and distractors by dopamine D1 receptors in primate prefrontal cortex. *Nature communications* **7**, 13218 (2016).
34. Glantz, L.A. & Lewis, D.A. Decreased dendritic spine density on prefrontal cortical pyramidal neurons in schizophrenia. *Arch Gen Psychiatry* **57**, 65-73 (2000).
35. Hof, P.R.*, et al.* Differential distribution of neurofibrillary tangles in the cerebral cortex of dementia pugilistica and Alzheimer's disease cases. *Acta Neuropathol* **85**, 23-30 (1992).
36. Woo, E., Sansing, L.H., Arnsten, A.F.T. & Datta, D. Chronic Stress Weakens Connectivity in the Prefrontal Cortex: Architectural and Molecular Changes. *Chronic stress* **5**, 24705470211029254 (2021).
37. Nandy, A.S., Sharpee, T.O., Reynolds, J.H. & Mitchell, J.F. The fine structure of shape tuning in area V4. *Neuron* **78**, 1102-1115 (2013).
38. Mitchell, J.F., Reynolds, J.H. & Miller, C.T. Active Vision in Marmosets: A Model System for Visual Neuroscience. *The Journal of Neuroscience* **34**, 1183-1194 (2014).
39. Krienen, F.M.*, et al.* A marmoset brain cell census reveals regional specialization of cellular identities. *Sci Adv* **9**, eadk3986 (2023).
40. Datta, D.*, et al.* Key Roles of CACNA1C/Cav1.2 and CALB1/Calbindin in Prefrontal Neurons Altered in Cognitive Disorders. *JAMA Psychiatry* (2024).
41. Yao, Z.*, et al.* A taxonomy of transcriptomic cell types across the isocortex and hippocampal formation. *Cell* **184**, 3222-3241 e3226 (2021).
42. Paspalas, C.D. & Goldman-Rakic, P.S. Microdomains for dopamine volume neurotransmission in primate prefrontal cortex. *J Neurosci* **24**, 5292-5300 (2004).
43. Paspalas, C.D. & Goldman-Rakic, P.S. Presynaptic D1 dopamine receptors in primate prefrontal cortex: target-specific expression in the glutamatergic synapse. *J Neurosci* **25**, 1260-1267 (2005).
44. Compte, A., Brunel, N., Goldman-Rakic, P.S. & Wang, X.J. Synaptic mechanisms and network dynamics underlying spatial working memory in a cortical network model. *Cereb Cortex* **10**, 910-923 (2000).
45. Znamenskiy, P.*, et al.* Functional specificity of recurrent inhibition in visual cortex. *Neuron* **112**, 991-1000.e1008 (2024).
46. Runyan, C.A.*, et al.* Response features of parvalbumin-expressing interneurons suggest precise roles for subtypes of inhibition in visual cortex. *Neuron* **67**, 847-857 (2010).

47. Wilson, D.E., *et al.* GABAergic Neurons in Ferret Visual Cortex Participate in Functionally Specific Networks. *Neuron* **93**, 1058-1065.e1054 (2017).
48. Yoshimura, Y. & Callaway, E.M. Fine-scale specificity of cortical networks depends on inhibitory cell type and connectivity. *Nat Neurosci* **8**, 1552-1559 (2005).
49. Wilson, D.E., Scholl, B. & Fitzpatrick, D. Differential tuning of excitation and inhibition shapes direction selectivity in ferret visual cortex. *Nature* **560**, 97-101 (2018).
50. Rao, S.G., Williams, G.V. & Goldman-Rakic, P.S. Isodirectional tuning of adjacent interneurons and pyramidal cells during working memory: evidence for microcolumnar organization in PFC. *J Neurophysiol* **81**, 1903-1916 (1999).
51. Wilson, F.A., O'Scalaidhe, S.P. & Goldman-Rakic, P.S. Functional synergism between putative gamma-aminobutyrate-containing neurons and pyramidal neurons in prefrontal cortex. *Proc Natl Acad Sci USA* **91**, 4009-4013 (1994).
52. Kuan, A.T., *et al.* Synaptic wiring motifs in posterior parietal cortex support decision-making. *Nature* **627**, 367-373 (2024).
53. Tanaka, S. Architecture and dynamics of the primate prefontal coritical circuit for spatial working memory. *Neural Networks* **12**, 1007-1020 (1999).
54. Xue, C. & Liu, F. Structured synaptic inhibition has a critical role in multiple-choice motion-discrimination tasks. *J Neurosci* **34**, 13444-13457 (2014).
55. Kroener, S., Chandler, L.J., Phillips, P.E. & Seamans, J.K. Dopamine modulates persistent synaptic activity and enhances the signal-to-noise ratio in the prefrontal cortex. *PLoS One* **4**, e6507 (2009).
56. Seamans, J.K., Durstewitz, D., Christie, B.R., Stevens, C.F. & Sejnowski, T.J. Dopamine D1/D5 receptor modulation of excitatory synaptic inputs to layer V prefrontal cortex neurons. *Proc Natl Acad Sci USA* **98**, 301-306 (2001).
57. Durstewitz, D., Seamans, J.K. & Sejnowski, T.J. Dopamine-mediated stabilization of delay-period activity in a network model of prefrontal cortex. *J Neurophysiol* **83**, 1733-1750 (2000).
58. Gonzalez-Burgos, G., Kroener, S., Seamans, J.K., Lewis, D.A. & Barrionuevo, G. Dopaminergic modulation of short-term synaptic plasticity in fast-spiking interneurons of primate dorsolateral prefrontal cortex. *J Neurophysiol.* **94**, 4168-4177 (2005).
59. Gao, W.J. & Goldman-Rakic, P.S. Selective modulation of excitatory and inhibitory microcircuits by dopamine. *Proc Natl Acad Sci USA* **100**, 2836-2841 (2003).
60. Williams, G.V. & Castner, S.A. Under the curve: critical issues for elucidating D1 receptor function in working memory. *Neuroscience* **139**, 263-276 (2006).
61. Lagzi, F. & Fairhall, A.L. Emergence of co-tuning in inhibitory neurons as a network phenomenon mediated by randomness, correlations, and homeostatic plasticity. *Sci Adv* **10**, eadi4350 (2024).
62. Suzuki, M. & Gottlieb, J. Distinct neural mechanisms of distractor suppression in the frontal and parietal lobe. *Nat Neurosci* **16**, 98-104 (2013).
63. Brozoski, T.J., Brown, R.M., Rosvold, H.E. & Goldman, P.S. Cognitive deficit caused by regional depletion of dopamine in prefrontal cortex of rhesus monkey. *Science* **205**, 929-932 (1979).
64. Sawaguchi, T. & Goldman-Rakic, P.S. D1 dopamine receptors in prefrontal cortex: involvement in working memory. *Science* **251**, 947-950 (1991).
65. Durstewitz, D. & Seamans, J.K. The dual-state theory of prefrontal cortex dopamine function with relevance to catechol-o-methyltransferase genotypes and schizophrenia. *Biol Psychiatry* **64**, 739-749 (2008).
66. Li, Y.C., Liu, G., Hu, J.L., Gao, W.J. & Huang, Y.Q. Dopamine D(1) receptor-mediated enhancement of NMDA receptor trafficking requires rapid PKC-dependent synaptic insertion in the prefrontal neurons. *J Neurochem* **114**, 62-73 (2010).
67. Paspalas, C.D., Wang, M. & Arnsten, A.F. Constellation of HCN channels and cAMP regulating proteins in dendritic spines of the primate prefrontal cortex: potential substrate for working memory deficits in schizophrenia. *Cereb Cortex* **23**, 1643-1654 (2013).

68. Brunel, N. & Wang, X.J. Effects of neuromodulation in a cortical network model of object working memory dominated by recurrent inhibition. *J Comput Neurosci* **11**, 63-85 (2001).
69. Froudist-Walsh, S.*, et al.* A dopamine gradient controls access to distributed working memory in the large-scale monkey cortex. *Neuron* **109**, 3500-3520 e3513 (2021).
70. Gao, W.J., Wang, Y. & Goldman-Rakic, P.S. Dopamine modulation of perisomatic and peridendritic inhibition in prefrontal cortex. *J Neurosci* **23**, 1622-1630 (2003).
71. Anastasiades, P.G., Boada, C. & Carter, A.G. Cell-Type-Specific D1 Dopamine Receptor Modulation of Projection Neurons and Interneurons in the Prefrontal Cortex. *Cereb Cortex* **29**, 3224-3242 (2019).
72. Furman, M. & Wang, X.J. Similarity effect and optimal control of multiple-choice decision making. *Neuron* **60**, 1153-1168 (2008).
73. Barbosa, J.*, et al.* Interplay between persistent activity and activity-silent dynamics in the prefrontal cortex underlies serial biases in working memory. *Nat Neurosci* **23**, 1016-1024 (2020).
74. Najafi, F.*, et al.* Excitatory and Inhibitory Subnetworks Are Equally Selective during Decision-Making and Emerge Simultaneously during Learning. *Neuron* **105**, 165-179.e168 (2020).
75. Roach, J.P., Churchland, A.K. & Engel, T.A. Choice selective inhibition drives stability and competition in decision circuits. *Nature communications* **14**, 147 (2023).
76. Wang, X.J., Tegner, J., Constantinidis, C. & Goldman-Rakic, P.S. Division of labor among distinct subtypes of inhibitory neurons in a cortical microcircuit of working memory. *Proc Natl Acad Sci USA* **101**, 1368-1373 (2004).
77. Lagzi, F., Bustos, M.C., Oswald, A.-M. & Doiron, B. Assembly formation is stabilized by Parvalbumin neurons and accelerated by Somatostatin neurons. *bioRxiv*, 2021.2009.2006.459211 (2021).
78. Torres-Gomez, S.*, et al.* Changes in the Proportion of Inhibitory Interneuron Types from Sensory to Executive Areas of the Primate Neocortex: Implications for the Origins of Working Memory Representations. *Cereb Cortex* **30**, 4544-4562 (2020).
79. Kvitsiani, D.*, et al.* Distinct behavioural and network correlates of two interneuron types in prefrontal cortex. *Nature* **498**, 363-366 (2013).
80. DeFelipe, J. Types of neurons, synaptic connections and chemical characteristics of cells immunoreactive for calbindin-D28K, parvalbumin and calretinin in the neocortex. *J Chem Neuroanat* **14**, 1-19 (1997).
81. Yang, G.R., Murray, J.D. & Wang, X.J. A dendritic disinhibitory circuit mechanism for pathway-specific gating. *Nature communications* **7**, 12815 (2016).
82. Krabbe, S.*, et al.* Adaptive disinhibitory gating by VIP interneurons permits associative learning. *Nat Neurosci* **22**, 1834-1843 (2019).
83. Dzaja, D., Hladnik, A., Bicanic, I., Bakovic, M. & Petanjek, Z. Neocortical calretinin neurons in primates: increase in proportion and microcircuitry structure. *Front Neuroanat* **8**, 103 (2014).
84. Finlay, J.M., Zigmond, M.J. & Abercrombie, E.D. Increased dopamine and norepinephrine release in medial prefrontal cortex induced by acute and chronic stress: effects of diazepam. *Neuroscience* **64**, 619-628 (1995).
85. Kodama, T., Hikosaka, K., Honda, Y., Kojima, T. & Watanabe, M. Higher dopamine release induced by less rather than more preferred reward during a working memory task in the primate prefrontal cortex. *Behav Brain Res* **266**, 104-107 (2014).
86. Arnsten, A.F.T. & Goldman, P.S. Stress impairs prefrontal cortex cognitive function in monkeys: role of dopamine. *Soc.Neurosci.Abstr.* **16** (1990).
87. Arnsten, A.F. & Goldman-Rakic, P.S. Noise stress impairs prefrontal cortical cognitive function in monkeys: evidence for a hyperdopaminergic mechanism. *Arch Gen Psychiatry* **55**, 362-368 (1998).
88. Arnsten, A.F.T., Cai, J.X., Murphy, B.L. & Goldman-Rakic, P.S. Dopamine D1 receptor mechanisms in the cognitive performance of young adult and aged monkeys. *Psychopharmacology* **116**, 143-151 (1994).

89. Murphy, B.L., Arnsten, A.F.T., Goldman-Rakic, P.S. & Roth, R.H. Increased dopamine turnover in the prefrontal cortex impairs spatial working memory performance in rats and monkeys. *Proc Natl Acad Sci USA* **93**, 1325-1329 (1996).
90. Ma, S.*, et al.* Molecular and cellular evolution of the primate dorsolateral prefrontal cortex. *Science*, eabo7257 (2022).
91. Robinson, M.D., McCarthy, D.J. & Smyth, G.K. edgeR: a Bioconductor package for differential expression analysis of digital gene expression data. *Bioinformatics* **26**, 139-140 (2009).

Supplementary Materials

Supplementary Figure 1

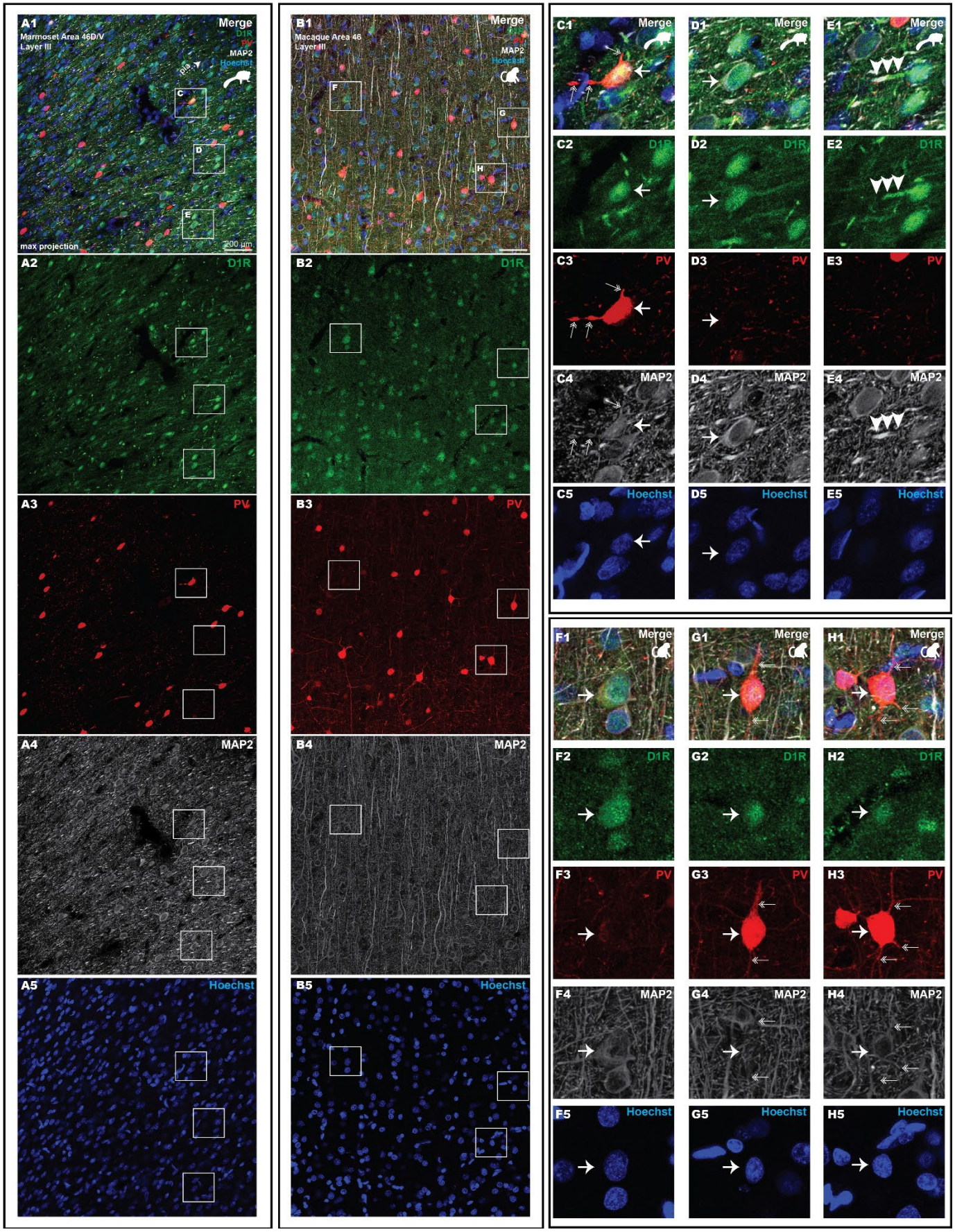

Figure S1 – Comparative multi-label immunofluorescence in layer III dlPFC for PV, D1R, MAP2, and Hoechst. Marmoset **(A1-5)** and macaque **(B1-5)** layer III dlPFC ***A1-A5,*** Layer III of marmoset A46D, labeled for PV (red), D1R (green), microtubule-associated protein 2 (MAP2, white), and the Hoechst nuclear stain (blue). White square insets are shown on the right. Apical dendrites were cut in oblique cross-section, distinguishable using MAP2 labeling **(A4)**, and are oriented toward Layer I in the direction of the upper right. Apical dendrites are also strongly labeled by the D1R antibody **(A2)**, and overlap with the MAP2 label (**E1**, **E2**, **E4**, white arrowheads). Macaque apical dendrites are oriented upward **(B1)**, and are strongly labeled by MAP2 **(B4)**, although their apical dendrites are labeled more weakly for D1R than in the marmoset **(B2)**. In general, PV neuronal processes were more prominently labeled in the macaque compared to the marmoset (**B3** vs. **B4**). ***C1-C5,*** A marmoset D1R positive PV neuron (white arrow). The PV soma and proximal PV processes (double-headed arrows) are also lightly labeled by MAP2 **(C4)**. Strong D1R labeling corresponds with the nucleus (**C2** vs. **C5**). ***D1-D5,*** A D1R positive pyramidal neuron (**D2**, white arrow) with an apical dendrite, stretching toward the left, in the marmoset. The soma and apical dendrite are also labeled strongly by MAP2 **(D4)**. Strongest D1R labeling was observed in the nucleus (**D2** vs. **D5**). ***E1-E5,*** A strongly labeled D1R segment (white arrowheads), which was common in the marmoset tissue, likely an obliquely cut apical dendrite. The D1R label **(E2)** overlaps and is continuous with the MAP2 label **(E4)**. ***F1-F5,*** A D1R positive pyramidal neuron **(F2)** in the macaque, with an apical dendritic segment reaching upwards toward Layer I. The neuron is also labeled by MAP2 **(F4)**. D1R labeling is strongest in the nuclear region (**F2** vs. **F5**). ***G1-G5,*** A macaque PV neuron **(G3)** with robust D1R labeling **(G2)**. The D1R labeling is strongest in what corresponds to the nuclear region (**G2** vs. **G5**). The PV neuron is negative for MAP2 **(G4)**. ***H1-H5,*** A macaque PV neuron **(H3)** lightly positive for D1R (white arrow). To its left is a PV neuron negative for D1R. The center PV neuron is positive for MAP2 **(H4)**, including proximal PV processes (double-headed arrows in **H2**, **H4**). Again, the D1R is strongest in the nuclear region (**H2** vs. **H5**).

Supplementary Figure 2

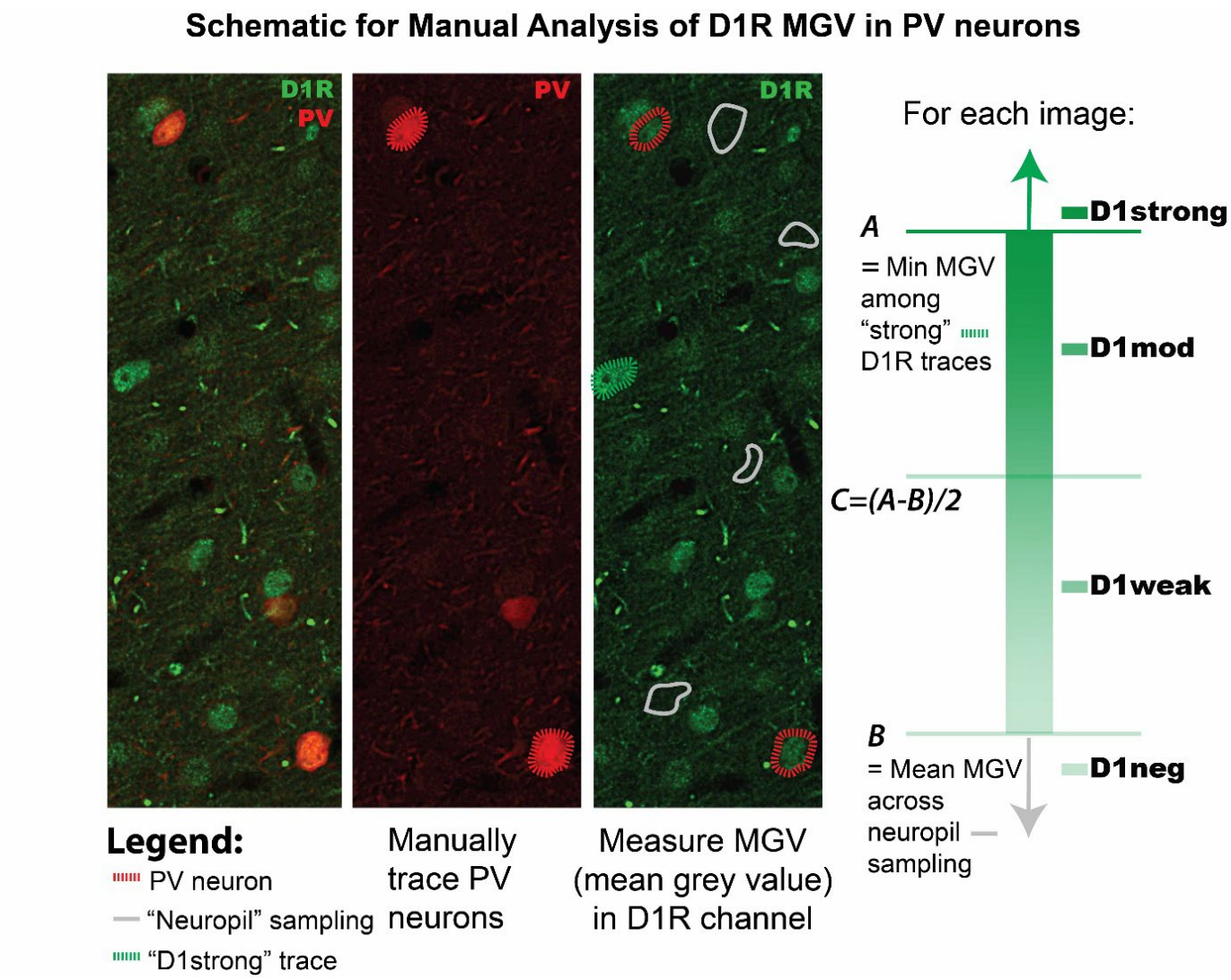

Figure S2 – Simplified exemplary schematic for manual comparative analysis of D1R expression levels in PV neurons. Single focal planes from z-stacks were extracted (left image). The PV channel was isolated (middle column, red), and the somata of PV neurons were traced (red dashed line). PV neurons not completely in plane were discarded (e.g., faint PV+ neuron in the middle of the image). In the isolated D1R channel (green, right image), strongly labeled D1R neurons were traced (dashed green line), as well as regions of "neuropil"-like immunonegative labeling (grey outlines). The mean grey value (MGV) of the D1R signal was measured in each type of trace. A binning strategy was used to classify PV traces (schematic at right). PV cells were deemed "D1neg" if their MGV fell below the average MGV from the sampled neuropil traces. PV cells were deemed "D1strong" if their average MGV exceeded the minimum from strongly labeled D1R cells in the image. PV cells in the intermediate bins were classified based on their average MGV falling between those two extremes. This analysis was performed for each image to ensure normalization based on the unique illumination level for each plane. Data obtained per image was then compiled across images by subject.

Supplementary Figure 3

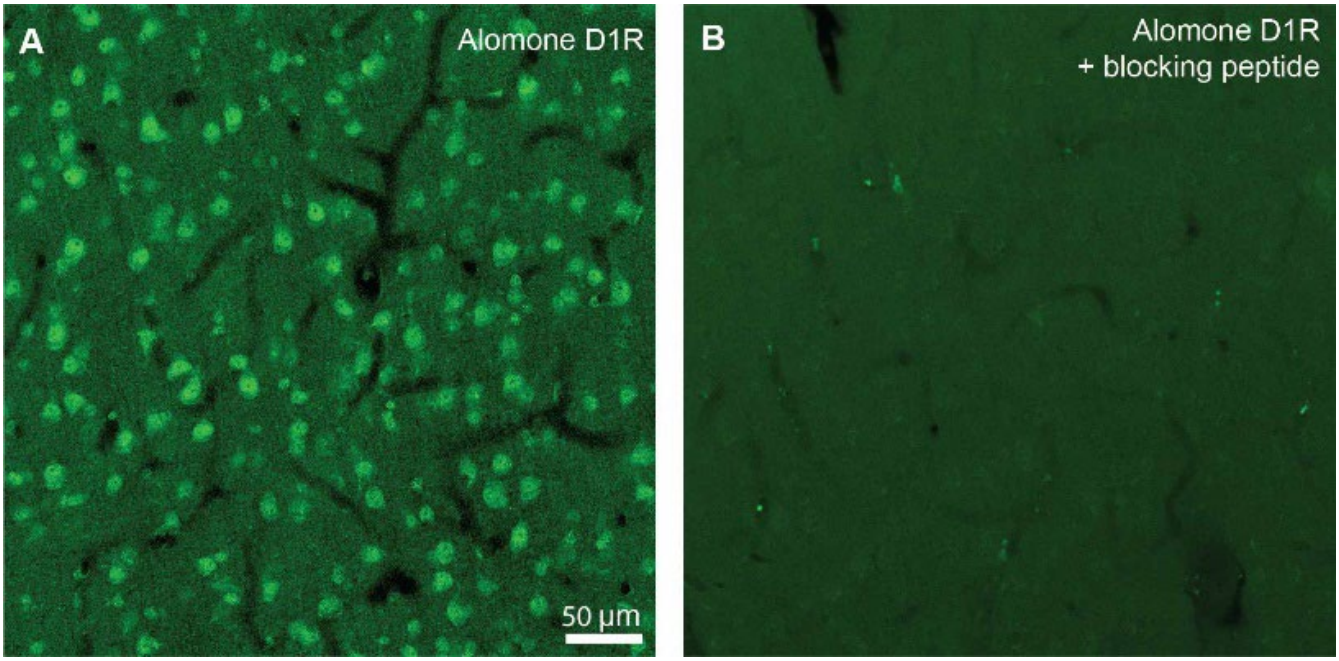

Figure S3 - Preadsorption Control for D1R antibody. ***A,*** Macaque dlPFC labeled with Alomone rabbit anti-D1R (cat# ADR-001). Strong labeling is visible particularly in pyramidal-like cells with apical dendrites oriented upwards toward Layer I. ***B,*** Test section using preadsorption control for primary antibody. Co-incubation of the primary antibody with the bespoke blocking peptide (Alomone, #BLP-DR001) produced negligible labeling.

Supplementary Figure 4

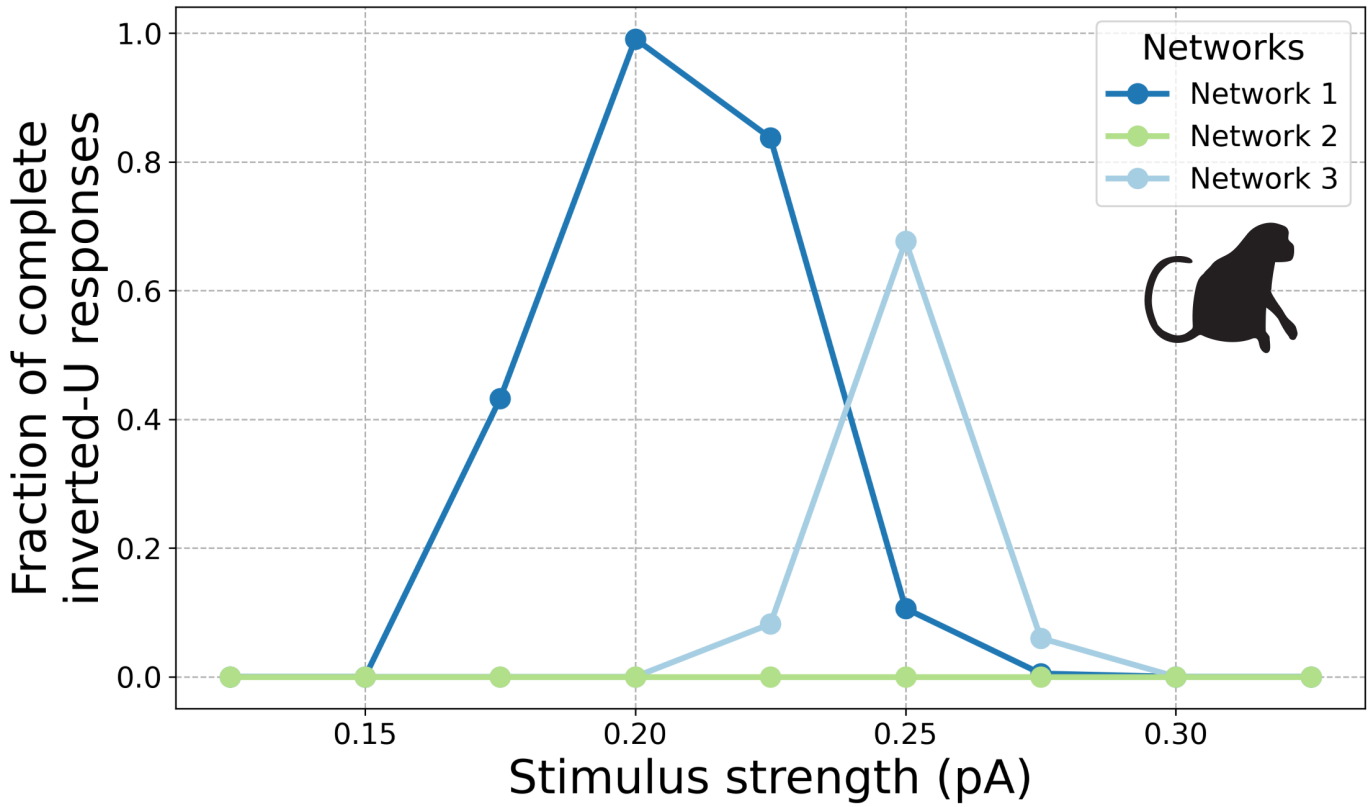

Figure S4 – D1R expression in I_{NEAR} cells facilitates the inverted-U response. The plot presents the fraction of complete inverted-U responses in the macaque, out of 1000 repetitions for each combination of cell type-specific D1R expression pattern (Networks 1-3), stimulus strength, and set of five D1R occupancy levels (no, low, mid, high, very high). A complete inverted-U involves (1) transient activity at no D1R occupancy, (2) any one of erroneous, noise- and distractor-resistant, or distractible persistent activity at low D1R occupancy, (3) noise- and distractor-resistant persistent activity at mid D1R occupancy, (4) distractible persistent activity at high D1R occupancy, and (5) transient activity at very high D1R occupancy. Network 1 could reproduce the inverted-U for approximately the 0.150-0.300 pA range of stimulus strengths, with a frequency of 0% for 0.150 pA, 43.2% for 0.175 pA, 99.1% for 0.200 pA, 83.7% for 0.225 pA, 10.6% for 0.250 pA, 0.5% for 0.275%, and 0% for 0.300 pA. Network 2 could not reproduce the inverted-U response at any stimulus strength. Network 3 could reproduce the inverted-U for approximately the 0.200-0.300 pA range of stimulus strengths, with a frequency of 0.0% for 0.200 pA, 8.2% for 0.225 pA, 67.7% for 0.250 pA, 6.0% for 0.275 pA, and 0% for 0.300 pA.

Supplementary Figure 5

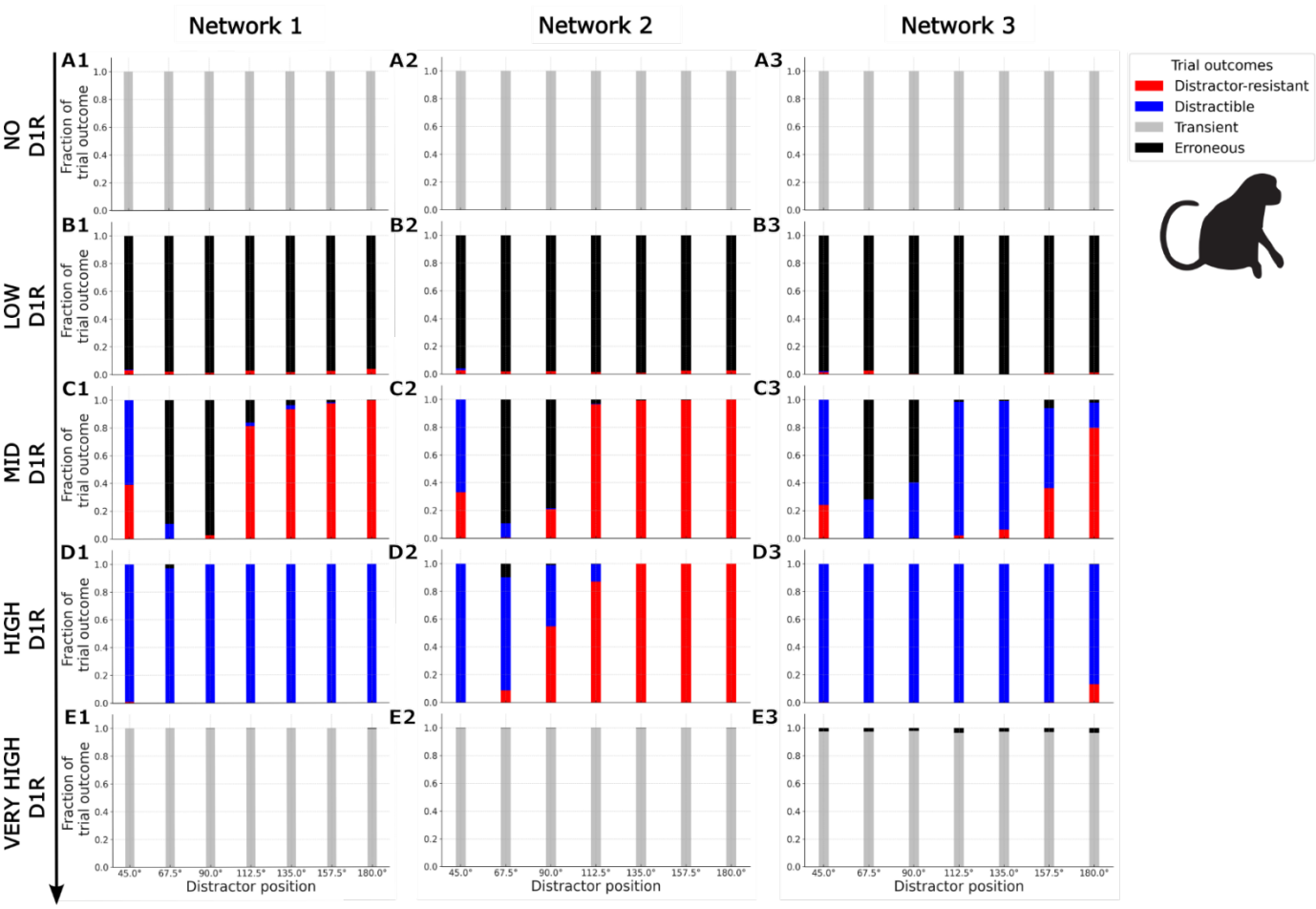

Figure S5 – Fraction of classified trial outcomes at different distractor positions across D1R occupancy levels for Networks 1, 2, and 3 in macaque. The strength of the stimuli is 0.2 pA for Network 1 and 2, and 0.25 pA for Network 3. ***A,*** At no D1R occupancy, Networks 1, 2, and 3 **(A1-3)** exhibit transient activity across distractor positions. ***B,*** At low D1R occupancy, all three networks **(B1-3)** overwhelmingly exhibit erroneous persistent activity across distractor positions, with some steady fraction of noise- and distractor-resistant persistent activity. ***C,*** At mid D1R occupancy, Networks 1 and 2 **(C1-2)** alike exhibit predominantly distractible persistent activity, but also a significant fraction of noise- and distractor-resistant persistent activity, at near distractor positions (45.0°). For both networks, erroneous persistent activity predominates at near-to-intermediate positions (67.5°-90.0°), with some decreasing fraction at intermediate-to-far positions (112.5°-180.0°). Both networks overwhelmingly exhibit noise- and distractor-resistant persistent activity at intermediate-to-far positions (112.5°-180.0°). Conversely, Network 3 **(C3)** predominantly exhibits distractible persistent activity at near (45.0°) and intermediate-to-far (112.5°-157.5°) positions, erroneous persistent activity at near-to-intermediate positions (67.5°-90.0°), and noise- and distractor-resistant persistent activity only at the farthest position (180.0°). Upon inspection of several individual example trials, the erroneous persistent activity at near-to-intermediate positions (67.5°-90.0°) across the networks appears to result from the persistent activity peak shifting to a position between the target and distractor during the distractor delay period. ***D,*** At high D1R occupancy, Networks 1 and 3 **(D1, D3)** overwhelmingly exhibit distractible persistent activity across distractor positions. Conversely, Network 2 **(D2)** exhibits overwhelmingly distractible persistent activity at near distractor positions (45.0°-67.5°), gradually switching to a robust noise- and distractor-resistant persistent activity regime at intermediate-to-far distractor positions (90.0°-180.0°). ***E,*** At very high D1R occupancy, all three networks **(E1-3)** overwhelmingly exhibit transient activity across distractor positions, with some fraction of erroneous persistent activity, especially in Network 3.

Supplementary Figure 6

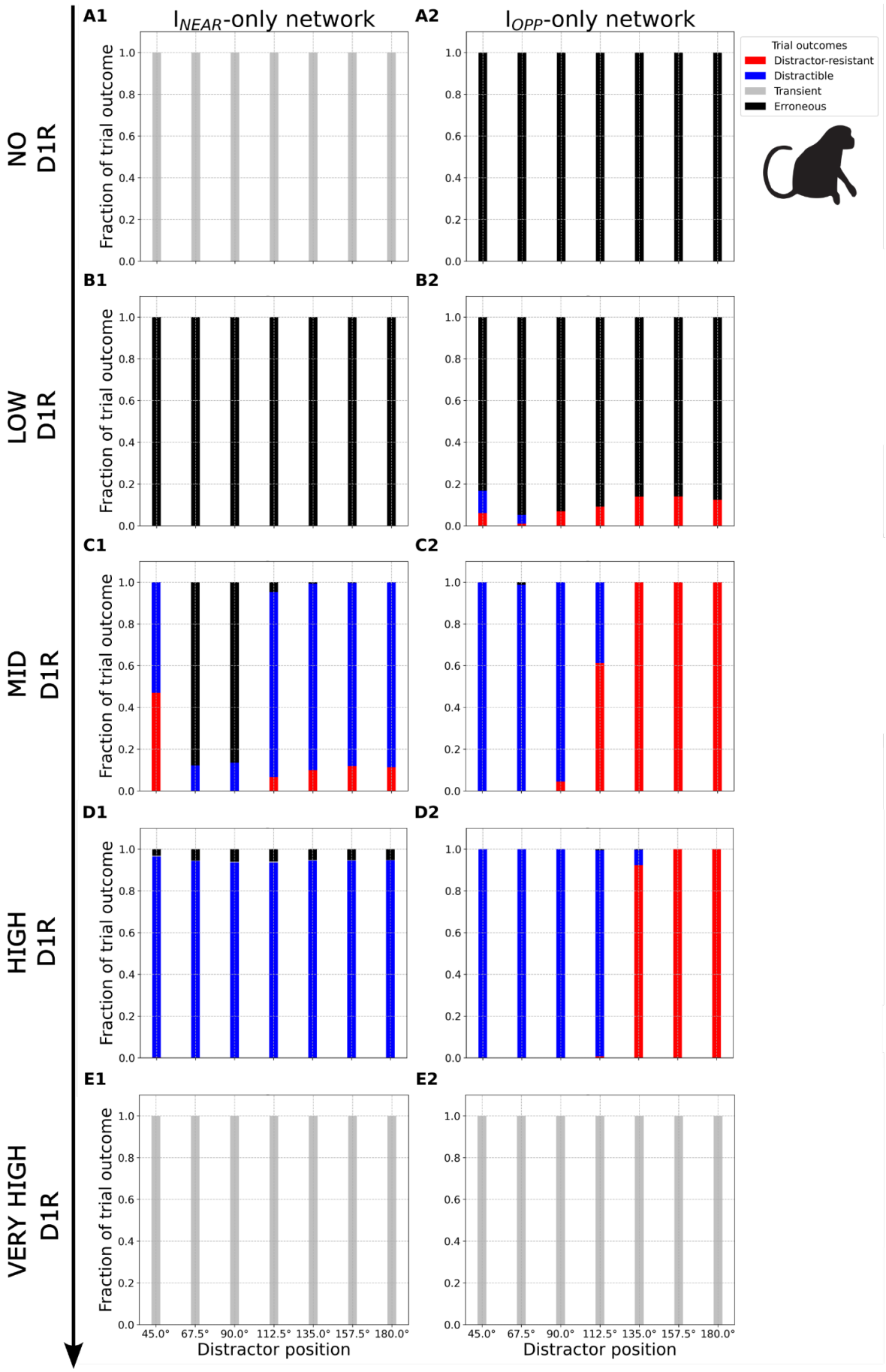

Figure S6 – Fraction of classified trial outcomes at different distractor positions across D1R occupancy levels for the I_{NEAR}-only and the I_{OPP}-only networks in macaque. The strength of the stimuli is 0.25 pA. ***A,*** At no D1R occupancy, the I_{NEAR}-only network **(A1)** exhibits transient activity across distractor positions. The I_{OPP}-only network **(A2)** exhibits erroneous persistent activity across distractor positions. Upon inspection of several individual example trials, the errors mainly consisted of stimulus-evoked persistent activity but only for the target or for the distractor, similar to the overinhibition errors at higher D1R occupancies in Networks 1-3. ***B,*** At low D1R occupancy, the I_{NEAR}-only network **(B1)** exhibits erroneous persistent activity across distractor positions. The I_{OPP}-only network **(B2)** also primarily exhibits erroneous persistent activity across distractor positions, but also some fractions of distractible persistent activity at near positions (45.0°-67.5°), as well as noise- and distractor-resistant persistent activity with fractions across distractor positions forming a discernible irregular amplitude sinusoidal pattern. ***C,*** At mid D1R occupancy, the I_{NEAR}-only network **(C1)** exhibits distractible persistent activity primarily at near (45.0°) and intermediate-to-far (112.5°-180°), but also some at near-to-intermediate (67.5°-90.0°), distractor positions. There is a significant fraction of noise- and distractor-resistant persistent activity at the near (45.0°) and some at the intermediate-to-far (112.5°-180°) positions. Notably, erroneous persistent activity predominates at near-to-intermediate positions (67.5°-90.0°), with some gradually decreasing fractions at intermediate-to-far positions (112.5°-180.0°). Qualitatively different, the I_{OPP}-only network **(C2)** overwhelmingly exhibits distractible persistent activity at near-to-intermediate positions (45.0°-90.0°), switching to a robust noise- and distractor-resistant persistent activity regime at intermediate-to-far positions (112.5°-180.0°). ***D,*** At high D1R occupancy, the I_{NEAR}-only network **(D1)** overwhelmingly exhibits distractible persistent activity, with some steady fraction of erroneous persistent activity, across distractor positions. Conversely, the I_{OPP}-only network **(D2)** exhibits overwhelmingly distractible persistent activity at near-to-intermediate positions (45.0°-112.5°), abruptly switching to a robust noise- and distractor-resistant persistent activity regime at intermediate-to-far positions (135.0°-180.0°). ***E,*** At very high D1R occupancy, both networks **(E1-2)** exhibit transient activity across distractor positions. Importantly, focusing on the typical, mid D1R occupancy, I_{NEAR}-only inhibition facilitates significant resistance to near distractor stimuli and noise activations (45°), while I_{OPP}-only inhibition – strong resistance to far distractor stimuli and noise activations (112.5°-180.0°). I_{OPP}-only inhibition also curbs errors at the near-to-intermediate distractor positions (67.5°-90.0°). However, a microcircuit with only I_{NEAR} or I_{OPP} cells seems dysfunctional due to overall poor distractor resistance across distractor positions expected at mid D1R occupancy in the former case and a lack of distractibility for far distractors expected at high D1R occupancy in the latter case.

Supplementary Figure 7

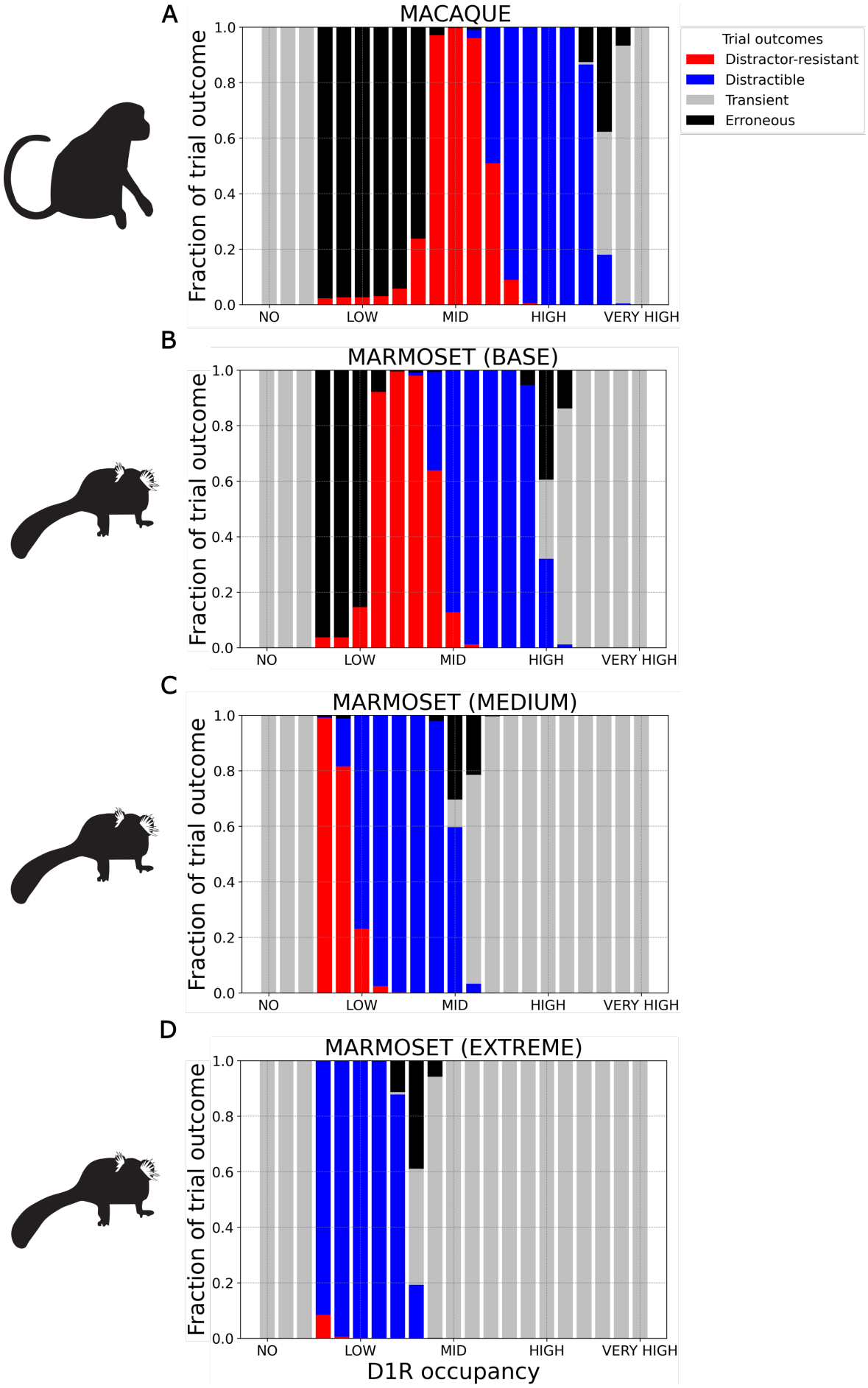

Figure S7 – Fraction of classified trial outcomes across the granulated D1R occupancy scale in the visuospatial working memory task with distractors presented only at 180° to Network 1 in macaque and the three cases of V_{th} sigmoid midpoint shift for marmoset. The strength of the stimuli is 0.2 pA. In the no D1R occupancy range, both species **(A-D)** show transient activity. In the low D1R occupancy range, the macaque **(A)** exhibits predominantly erroneous persistent activity, while the base marmoset case **(B)** transitions from the erroneous to the noise- and distractor-resistant persistent activity regime, the medium marmoset case **(C)** transitions from the noise- and distractor-resistant to the distractible persistent activity regime, and the extreme marmoset case **(D)** exhibits predominantly distractible persistent activity. In the mid D1R occupancy range, the macaque **(A)** overwhelmingly exhibits noise- and distractor-resistant persistent activity. The base marmoset case **(B)** transitions to the distractible persistent activity regime, with a decreasing fraction of noise- and distractor-resistant persistent activity. The medium marmoset case **(C)**, transitions to transient activity, with a decreasing fraction of distractible persistent activity and a significant fraction of erroneous persistent activity. The extreme marmoset case **(D)**, which predominantly exhibits transient activity. In the high D1R occupancy range, the macaque **(A)** exhibits a robust distractible persistent activity regime, while the base marmoset case **(B)** transitions from the distractible persistent activity to the transient activity regime, with a significant fraction of erroneous persistent activity, and the medium and extreme marmoset cases **(C-D)** exhibit transient activity. Finally, in the very high D1R occupancy range, both species **(A-D)** settle into a transient activity regime. Notably, as the shift increases across the marmoset cases, the range of D1R occupancies which can support persistent activity decreases.